$$e^T|\Psi_0\rangle$$

CCSD(T)-F12
S66x8

$$\left\{-\tfrac{1}{2}\nabla^2 + V_{KS}[\rho]\right\} = |\phi_i\rangle$$

Showcasing research from the laboratory of Professor Jan Martin at the Department of Organic Chemistry, Weizmann Institute of Science, Reḥovot, Israel

Title: The S66x8 benchmark for noncovalent interactions revisited: explicitly correlated *ab initio* methods and density functional theory

The Martin group at Weizmann combines rigorous wavefunction *ab initio* methods (such as the Weizmann-n or Wn family) with development, validation, and application of density functional approaches. Their chemical interests focus on organometallic chemistry and catalysis, but recently are branching out in the direction of biomolecules and noncovalent interactions.

Research in the Kozuch group at Ben-Gurion University focuses on catalysis, tunneling effects on kinetics, and the nature of the chemical bond.
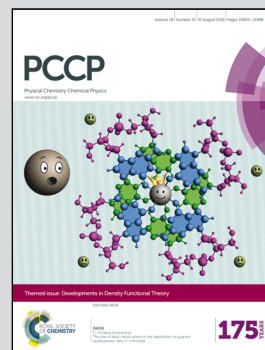
ROYAL SOCIETY OF CHEMISTRY

www.rsc.org/pccp

The S66x8 benchmark for noncovalent interactions revisited: explicitly correlated *ab initio* methods and density functional theory†

Brina Brauer,‡[a] Manoj K. Kesharwani,‡[a] Sebastian Kozuch[b] and Jan M. L. Martin★[a]

The S66x8 dataset for noncovalent interactions of biochemical relevance has been re-examined by means of MP2-F12 and CCSD(F12*)(T) methods. We deem our revised benchmark data to be reliable to about 0.05 kcal mol^{-1} RMS. Most levels of DFT perform quite poorly in the absence of dispersion corrections: somewhat surprisingly, that is even the case for the double hybrids and for dRPA75. Analysis of optimized D3BJ parameters reveals that the main benefit of dRPA75 and DSD double hybrids alike is the treatment of midrange dispersion. dRPA75-D3BJ is the best performer overall at RMSD = 0.10 kcal mol^{-1}. The nonlocal VV10 dispersion functional is especially beneficial for the double hybrids, particularly in DSD-PBEP86-NL (RMSD = 0.12 kcal mol^{-1}). Other recommended dispersion-corrected functionals with favorable price/performance ratios are ωB97X-V, and, surprisingly, B3LYP-D3BJ and BLYP-D3BJ (RMSDs of 0.23, 0.20 and 0.23 kcal mol^{-1}, respectively). Without dispersion correction (but parametrized for midrange interactions) M06-2X has the lead (RMSD = 0.45 kcal mol^{-1}). A collection of three energy-based diagnostics yields similar information to an SAPT analysis about the nature of the noncovalent interaction. Two of those are the percentages of Hartree−Fock and of post-MP2 correlation effects in the interaction energy; the third, CSPI = $[IE_{ss}^{(2)} - IE_{ab}^{(2)}]/[IE_{ss}^{(2)} + IE_{ab}^{(2)}]$ or its derived quantity DEBC = CSPI/$(1 + CSPI^2)^{1/2}$, describes the character of the MP2 correlation contribution, ranging from 0 (purely dispersion) to 1 (purely other effects). In addition, we propose an improved, parameter-free scaling for the (T) contribution based on the E_{corr}[CCSD-F12b]/E_{corr}[CCSD] and E_{corr}[CCSD(F12*)]/E_{corr}[CCSD] ratios. For Hartree−Fock and conventional DFT calculations, full counterpoise generally yields the fastest basis set convergence, while for double hybrids, half-counterpoise yields faster convergence, as previously established for correlated *ab initio* methods.

Introduction

Noncovalent interactions have great importance in many areas of research, particularly in chemistry and biological science.[1,2] In biomolecules, noncovalent interactions play a major role in determining their structure and reactivity: hydrogen bonding, π stacking, and dispersion interactions are among the most important noncovalent interactions.

All present-day computational methods capable of handling biomolecules with thousands of atoms, such as molecular mechanics force fields (*e.g.* ref. 3) and semiempirical methods (*e.g.*, ref. 4 and 5), are highly approximated and heavily parametrized. Ideally, parametrization of such approximate methods would be based on experimental observations; in practice, this is an intractable problem as experimental data are not available in sufficient quantity or in isolation from various environmental or dynamical effects that cannot easily be included in the approximate method during the many evaluation cycles required for parametrization. Highly accurate *ab initio* computational data represent a convenient alternative.

From a SAPT (symmetry-adapted [intermolecular] perturbation theory) perspective (see ref. 6–8 for recent reviews), the interaction energy of a noncovalent dimer can be decomposed into four main components: exchange repulsion (E_{exc}), electrostatic attraction (E_{elst}), induced electrostatic interactions (E_{ind}), and dispersion forces (E_{disp}). The balance of their relative importance changes between different types of systems,[9] as well as with distance, but dispersion (which is a long-range electron correlation effect) matters in all of them: indeed, in certain systems (such as noble

[a] Department of Organic Chemistry, Weizmann Institute of Science, 76100 Reḥovot, Israel. E-mail: gershom@weizmann.ac.il; Fax: +972 8 934 3029

[b] Department of Chemistry, Ben-Gurion University of the Negev, 84105 Beer-Sheva, Israel

† Electronic supplementary information (ESI) available: Spreadsheet with revised reference interaction energies for the S66x8 dataset, interaction energies at various levels of theory and SAPT results; Cartesian coordinates (66 structures, XMol .xyz format) for the interpolated minimum geometries. See DOI: 10.1039/c6cp00688d
‡ Equally contributing first authors.

This journal is © the Owner Societies 2016

Phys. Chem. Chem. Phys., 2016, **18**, 20905–20925 | 20905

gas dimers or alkane dimers) it is the glue that holds the dimer together at all. Electron correlation however also contributes in higher order to induced and electrostatic forces, particularly at shorter distances. To sum up, no accurate treatment of long-range correlation effects is possible without accounting for electron correlation.[10]

Coupled-cluster correlated methods with sufficiently large basis sets are known to accurately reproduce these interactions, but their high computational cost and massive resource demands limit their use to small benchmark systems.

Such benchmark data, for a representative set of small systems, do enable the validation and/or calibration of less demanding, more approximate methods, such as density functional theory.

In the past decade, a number of databases have been proposed for noncovalent interactions. An early one that has been used in the parametrization of a number of empirical density functionals is S22,[11] which are 22 noncovalent complexes ranging from water and methane dimers to the adenine–thymine base pair (both Watson–Crick and stacked). Its *ab initio* reference data were recently comprehensively revised.[12]

In order to have a broader set that is more representative of interactions one might see in biomolecules, Hobza and coworkers assembled a larger S66 set[9,13] of 66 noncovalent pairs, generated from 14 monomers in various combinations. The selection of monomers was based on their frequency as motifs or functional groups in the most commonly found biomolecules. The S66 set was designed with a balance in mind between electrostatic dominated (hydrogen bonding), dispersion dominated (including π stacking), and mixed-influenced complexes. Single hydrogen bonds, aromatic–aliphatic, and aliphatic–aliphatic interactions are also incorporated into the S66 set, which were not adequately covered by the narrower S22 dataset.

In an actual biomolecule, such interactions would not necessarily occur near the equilibrium inter-monomer separation, but at the separation dictated by the geometry of the system (*e.g.*, by the secondary structure of the protein). Hence, the Hobza group extended the S66 set by considering each dimer at eight different inter-monomer separations: $0.90r_e$, $0.95r_e$, r_e, $1.05r_e$, $1.10r_e$, $1.25r_e$, $1.5r_e$, and $2r_e$, where r_e is the equilibrium distance (the monomers were separated out without further geometry optimization). Thus, the S66x8 dataset was created, which is the subject of the present investigation. A full listing of the systems, together with the final recommended values obtained in the present work, is presented in Table 1. Reference geometries were taken "as is" from the Benchmark Energy and Geometry Database (www.begdb.com).[14]

Several studies have been published regarding the performance of lower *ab initio*, DFT and double-hybrid DFT methods using S66 and/or S66x8 as a benchmark.[15–20] Those results use the originally reported CCSD(T)/CBS calculated interaction energies as the reference. Those were based on extrapolated MP2 limits combined with additive "high-level corrections" (HLCs) – that is, CCSD(T)-MP2 differences – in the meager aug-cc-pVDZ basis set. Hobza and coworkers[13] re-evaluated the HLCs for just S66 (which is almost, but not quite, equivalent to the $1.0r_e$ 'slice' of S66x8): the RMSD (root mean square difference) between the original[9] and revised[13] sets is 0.10 kcal mol^{-1},

with the individual largest positive difference of 0.32 kcal mol^{-1} for acetic acid dimer, and largest negative difference of 0.12 kcal mol^{-1} for benzene-uracil. While this may not sound like a great deal, we shall show below that this is comparable with the accuracy of the best DFT methods available nowadays.

In reference to originally reported S66 and S66x8 database, Grimme and coworkers[17] have assessed the performance of several DFT methods, also have tested their own developed dispersion-correction schemes DFT-D3 and DFT-D3BJ. Aragó *et al.*[15] and Yu[16] have considered the S66 database to evaluate the efficacy of nonlocal van der Waals corrections for the double-hybrid DFT and spin-component-scaled double-hybrid DFT methods, respectively. The Hobza group[18] themselves have evaluated the performance of the MP2 variants for noncovalent interactions of the S66 benchmark set.

Basis set convergence of orbital-based CCSD(T) is quite slow, debilitatingly so in fact, for our purposes. Explicitly correlated[21,22] (in practice nowadays, F12)[23] approaches offer succor here: for many applications, we can expect a gain of 2–3 angular momentum steps.[24–26] Furthermore,[26,27] it has been reported that the combination of cc-pVDZ-F12 HLCs (high-level corrections, defined as the CCSD(T)-F12–MP2-F12 difference) with larger-basis MP2-F12 energetics yields excellent results for noncovalent interactions.

In this paper, we are reporting a revision of the reference interaction energies for the S66x8 dataset by means of explicitly correlated MP2 and coupled cluster methods. These interaction energy data will then be used to evaluate the performance of various wavefunction *ab initio* and density functional, as well as double-hybrid density functionals, which are fifth-rung DFT functionals from one perspective and occupy the twilight zone between wavefunction and DFT methods from another. In most cases, performance of DFT methods for noncovalent interactions is very poor unless dispersion corrections are included: both molecular mechanics-like corrections and nonlocal dispersion functionals will be considered in this work. The issue of BSSE (basis set superposition error) for explicitly correlated methods was considered in an earlier study[26] and will be re-examined here for all methods.

Computational details

All calculations were performed on the Faculty of Chemistry cluster at the Weizmann Institute of Science. Most wavefunction-based *ab initio* calculations were carried out using MOLPRO 2012.1,[28] while Turbomole[29] 6.6 was employed for some MP3-F12 calculations. The density functional calculations were performed using either the Gaussian 09 Rev. D.01 package,[30] or primarily for the double hybrids a locally modified version of ORCA.[31] The latter was primarily used for the double hybrids, owing to the availability of the RI-MP2 (resolution of the identity MP2) method,[32,33] approximation for the MP2-like step.

For conventional, orbital-based, *ab initio* calculations we mostly employed correlation-consistent[34–37] basis sets. In general, we combined diffuse-function augmented sets aug-cc-pVnZ

20906 | *Phys. Chem. Chem. Phys.*, 2016, **18**, 20905–20925

This journal is © the Owner Societies 2016

Table 1 Systems in the S66x8 dataset and final recommended dissociation energies (kcal mol^{-1}) obtained in the present work

	$0.90r_e$	$0.95r_e$	$1.00r_e$	$1.05r_e$	$1.10r_e$	$1.25r_e$	$1.50r_e$	$2.00r_e$
Hydrogen bonding								
01 water···water	4.659	4.954	4.951	4.768	4.487	3.473	2.113	0.872
02 water···MeOH	5.293	5.630	5.634	5.434	5.119	3.967	2.394	0.955
03 water···MeNH$_2$	6.577	6.937	6.929	6.689	6.315	4.932	2.982	1.143
04 water···peptide	7.748	8.149	8.153	7.907	7.514	6.023	3.844	1.442
05 MeOH···MeOH	5.396	5.787	5.824	5.644	5.337	4.172	2.538	1.015
06 MeOH···MeNH$_2$	7.067	7.550	7.603	7.385	7.005	5.517	3.352	1.277
07 MeOH···peptide	7.784	8.270	8.330	8.116	7.737	6.228	3.668	1.104
08 MeOH···water	4.684	5.032	5.063	4.901	4.629	3.611	2.208	0.909
09 MeNH$_2$···MeOH	2.862	3.078	3.063	2.917	2.704	1.984	1.104	0.396
10 MeNH$_2$···MeNH$_2$	3.724	4.113	4.165	4.016	3.756	2.793	1.309	0.390
11 MeNH$_2$···peptide	5.009	5.409	5.453	5.277	4.976	3.230	1.413	0.460
12 MeNH$_2$···water	6.834	7.272	7.300	7.070	6.688	5.234	3.158	1.199
13 peptide···MeOH	5.811	6.224	6.278	6.109	5.810	4.646	2.970	1.315
14 peptide···MeNH$_2$	6.938	7.446	7.536	7.360	7.021	5.639	3.567	1.498
15 peptide···peptide	8.204	8.696	8.767	8.569	8.204	6.728	4.457	1.793
16 peptide···water	4.801	5.150	5.191	5.044	4.790	3.825	2.468	1.139
17 uracil···uracil (BP)	16.229	17.358	17.583	17.214	16.473	13.350	8.462	3.380
18 water···pyridine	6.527	6.918	6.928	6.701	6.336	4.965	3.026	1.195
19 MeOH···pyridine	6.944	7.445	7.520	7.324	6.963	5.525	3.403	1.343
20 AcOH···AcOH	17.970	19.228	19.469	19.049	18.219	14.736	9.289	3.611
21 AcNH$_2$···AcNH$_2$	15.335	16.375	16.559	16.188	15.476	12.544	8.054	3.020
22 AcOH···uracil	18.421	19.632	19.877	19.488	18.697	15.325	9.953	4.179
23 AcNH$_2$···uracil	18.182	19.310	19.557	19.217	18.501	15.386	10.320	4.691
π stacking								
24 benzene···benzene (π–π)	0.105	2.016	2.725	2.813	2.607	1.578	0.515	0.072
25 pyridine···pyridine (π–π)	1.201	3.111	3.809	3.865	3.607	2.396	0.990	0.246
26 uracil···uracil (π–π)	7.976	9.640	9.976	9.590	8.848	6.217	3.196	1.034
27 benzene···pyridine (π–π)	0.602	2.636	3.358	3.414	3.159	2.012	0.752	0.155
28 benzene···uracil (π–π)	3.492	5.222	5.741	5.604	5.144	3.363	1.412	0.271
29 pyridine···uracil (π–π)	3.679	6.170	6.847	6.637	6.039	3.937	1.824	0.552
30 benzene···ethene	0.111	1.027	1.350	1.366	1.237	0.692	0.183	0.006
31 uracil···ethene	2.519	3.209	3.365	3.235	2.966	2.009	0.951	0.262
32 uracil···ethyne	2.708	3.507	3.702	3.571	3.281	2.232	1.054	0.278
33 pyridine···ethene	0.765	1.541	1.808	1.799	1.651	1.030	0.374	0.049
London dispersion complexes								
34 pentane···pentane	2.919	3.674	3.820	3.651	3.337	2.257	1.066	0.278
35 neopentane···pentane	1.913	2.542	2.651	2.518	2.282	1.516	0.711	0.191
36 neopentane···neopentane	1.484	1.758	1.790	1.698	1.551	1.060	0.512	0.139
37 cyclopentane···neopentane	1.669	2.299	2.443	2.354	2.161	1.482	0.716	0.194
38 cyclopentane···cyclopentane	2.301	2.894	3.038	2.893	2.621	1.731	0.804	0.211
39 benzene···cyclopentane	2.143	3.243	3.584	3.492	3.193	2.094	0.918	0.199
40 benzene···neopentane	1.859	2.683	2.909	2.824	2.591	1.729	0.786	0.196
41 uracil···pentane	3.932	4.792	4.934	4.689	4.163	2.508	1.012	0.228
42 uracil···cyclopentane	3.146	4.062	4.221	4.001	3.615	2.352	1.052	0.263
43 uracil···neopentane	2.954	3.684	3.782	3.566	3.217	2.102	0.955	0.244
44 ethene···pentane	1.647	1.966	1.987	1.861	1.674	1.093	0.497	0.123
45 ethyne···pentane	1.045	1.563	1.698	1.638	1.490	0.966	0.421	0.098
46 peptide···pentane	3.814	4.264	4.298	4.096	3.775	2.662	1.212	0.298
Mixed influence complexes								
47 benzene···benzene (TS)	1.657	2.603	2.898	2.853	2.643	1.804	0.856	0.237
48 pyridine···pyridine (TS)	2.547	3.336	3.566	3.489	3.255	2.328	1.206	0.384
49 benzene···pyridine (TS)	2.099	3.064	3.354	3.291	3.056	2.134	1.075	0.345
50 benzene···ethyne (CH-π)	1.847	2.636	2.865	2.800	2.593	1.802	0.903	0.277
51 ethyne···ethyne (TS)	1.203	1.464	1.516	1.456	1.341	0.934	0.463	0.135
52 benzene···AcOH (OH-π)	4.002	4.613	4.737	4.583	4.283	3.156	1.722	0.564
53 benzene···AcNH$_2$ (NH-π)	3.849	4.320	4.408	4.270	4.008	3.005	1.668	0.492
54 benzene···water (OH-π)	2.766	3.186	3.250	3.121	2.896	2.105	1.160	0.419
55 benzene···MeOH (OH-π)	3.403	4.014	4.168	4.057	3.804	2.813	1.542	0.526
56 benzene···MeNH$_2$ (NH-π)	2.457	3.051	3.209	3.109	2.861	1.960	0.951	0.267
57 benzene···peptide (NH-π)	3.756	4.978	5.313	5.183	4.825	3.458	1.837	0.632
58 pyridine···pyridine (CH-N)	2.989	3.970	4.259	3.973	3.517	2.226	1.041	0.287
59 ethyne···water (CH-O)	2.608	2.873	2.907	2.807	2.634	2.003	1.182	0.461
60 ethyne···AcOH (OH-π)	4.364	4.844	4.908	4.727	4.414	3.263	1.776	0.559
61 pentane···AcOH	2.741	2.938	2.913	2.761	2.544	1.812	0.802	0.177
62 pentane···AcNH$_2$	3.193	3.538	3.540	3.353	3.072	2.140	1.061	0.283
63 benzene···AcOH	2.691	3.581	3.798	3.660	3.354	2.260	1.040	0.271

Table 1 (continued)

	0.90r_e	0.95r_e	1.00r_e	1.05r_e	1.10r_e	1.25r_e	1.50r_e	2.00r_e
64 peptide···ethene	2.599	2.952	2.994	2.862	2.641	1.869	0.890	0.194
65 pyridine···ethyne	3.701	4.048	4.104	3.980	3.755	2.888	1.694	0.627
66 MeNH$_2$···pyridine	3.435	3.870	3.964	3.852	3.623	2.724	1.516	0.502

(n = D, T, Q, 5) on nonhydrogen atoms with the underlying regular cc-pVnZ basis sets on hydrogen. This practice has been denoted variously in the literature as aug′-cc-pVnZ by Del Bene,[38] A′VnZ by ourselves, ha*n*Z ("heavy-augmented") by the Hobza group,[13] heavy-aug-cc-pVnZ by the Sherrill group,[39] and (with a calendric pun) jul-cc-pVnZ by Papajak & Truhlar.[40]

For some of the *ab initio* calculations, and all of the DFT calculations, we employed the Weigend–Ahlrichs basis sets[41] def2-QZVP, def2-TZVPP, def2-TZVP and def2-SVP, as well as the diffuse-function augmented def2-QZVPD basis set.[42] In ORCA, we employed the corresponding auxiliary basis sets[43] for simultaneously fitting Coulomb and exchange, and the associated RI-MP2 auxiliary basis sets[44] for the double-hybrid calculations in ORCA. The Weigend–Ahlrichs family seeks to strike a balance between the requirements of DFT and wavefunction *ab initio* calculations, and was therefore deemed especially appropriate for the double hybrids.

Single-point explicitly correlated CCSD(T)(F12*), CCSD(T)-F12b and RI-MP2-F12 calculations were carried out using the cc-pVnZ-F12 (where n = D, T, Q) basis sets of Peterson *et al.*[45] in conjunction with the associated auxiliary and complementary auxiliary (CABS) basis sets.[46,47] The cc-pVnZ-F12 family was specifically developed with explicitly correlated calculations.

For some calibration calculations, the even larger cc-pV5Z-F12 basis set[27] was employed, which effectively corresponds to the basis set limit. Here, we employed a combination of Weigend's aug-cc-pV5Z/JKFIT basis set[43] for the Coulomb and exchange elements and Hättig's aug-cc-pwCV5Z/MP2FIT basis set[44] for both the RI-MP2 parts and for the CABS.

As recommended in ref. 48, the geminal exponents were set to β = 0.9 for cc-pVDZ-F12 and β = 1.0 for cc-pVTZ-F12 and cc-pVQZ-F12; for cc-pV5Z-F12 we used β = 1.2 as specified in ref. 27. The SCF component was improved through the "CABS correction".[49,50]

For the (T) term, which does not benefit from the F12, we considered three different corrections for basis set expansion: (a) the Marchetti–Werner approximation,[51,52] denoted CCSD(T*)-F12b, in which the (T) contribution is scaled by the E_{corr}[MP2-F12]/E_{corr}[MP2] correlation energy ratio; (b) analogues, denoted CCSD(Tb) and CCSD(Tc), in which the respective E_{corr}[CCSD-F12b]/E_{corr}[CCSD] and E_{corr}[CCSD(F12*)]/E_{corr}[CCSD] ratios were substituted; and (c) uniform scaling of the (T) contributions, denoted CCSD(Ts)-F12b,[27] in which the (T) contributions are multiplied by constant scaling factors of 1.1413 for cc-pVDZ-F12 and 1.0527 for cc-pVTZ-F12 (Table 3 in ref. 27). Options (a) and (b) are not strictly size-consistent, but can be rendered so by applying the dimer E_{corr}[MP2-F12]/E_{corr}[MP2], E_{corr}[CCSD-F12b]/E_{corr}[CCSD], *viz.* E_{corr}[CCSD(F12*)]/E_{corr}[CCSD] ratios also to the monomers: this is indicated by the notation CCSD(T*$_{sc}$), CCSD(Tb$_{sc}$), and CCSD(Tc$_{sc}$), respectively.

As byproducts of the MP2 and MP2-F12 calculations, we also obtain spin-component-scaled varieties such as SCS-MP2-F12,[53–55] SCS(MI)MP2, and S2-MP2.[56]

The following DFT functionals were considered (grouped by rung on the Perdew[57] "Jacob's Ladder"):
- on the second (GGA) rung, BP86,[58,59] BLYP,[58,60] and PBE;[61]
- on the third (meta-GGA) rung, TPSS,[62] and M06L;[63]
- on the fourth (occupied-orbital dependent) rung, the hybrid[64] functionals B3LYP,[60,65,66] B3PW91,[65,67] PBE0,[68] TPSS0,[69,70] APF,[71] M06,[63] and M06-2X;[63] as well as the range-separated hybrids M11,[72] CAM-B3LYP,[73] LC-ωPBE,[74] ωB97X-D3,[75] and ωB97X-V.[76]
- and on the fifth (virtual-orbital dependent) rung, the double hybrids B2PLYP,[77] B2GP-PLYP,[78] and the spin component scaled double hybrids DSD-PBEP86,[79] DSD-PBEPBE,[80] and DSD-PBEB95[80] methods. The dRPA75 method[81] represents approaches with correlation based on the random phase approximation (RPA).[82]

Further, we have also considered the following types of empirical dispersion corrections (for a review see ref. 83) for DFT energies:

(a) Grimme's 2006 version, denoted by the suffix "-D2" using Grimme's expression

$$E_{disp} = -s_6 \sum_{i=1}^{N_{at}-1} \sum_{j=i+1}^{N_{at}} \frac{C_6^{ij}}{R_{ij}^6} f_{dmp}(R_{ij}) \tag{1}$$

in which the damping function is taken as

$$f_{dmp}(R_{ij}) = \left[1 + \exp\left(-\alpha \left(\frac{R_{ij}}{s_R R_r} - 1 \right) \right) \right]^{-1} \tag{2}$$

where s_6 is a scaling factor that depends only of the functional used, $C_6^{ij} \approx (C_6^i C_6^j)^{1/2}$ is the dispersion coefficient for the atom pair *ij* computed by using a geometric mean, $R_r = R_{vdW,i} + R_{vdW,j}$ is the sum of the van der Waals radii of the two atoms in question, and specific numerical values for the atomic Lennard-Jones constants C_6^i and the van der Waals radii have been taken from ref. 84. The length-scaling factor s_R = 1.0 and hysteresis exponent α = 20.0 were set as in ref. 85.

(b) Grimme's DFT-D3[86,87] version with Becke–Johnson damping, denoted by the suffix "-D3BJ"

$$E_{disp}^{D3(BJ)} = -\sum_{i>j} s_6 \frac{C_{6,ij}}{R_{ij}^6 + [f(R_r)]^6} + s_8 \frac{C_{8,ij}}{R_{ij}^8 + [f(R_r)]^8} \tag{3}$$

in which $f(R_r) = a_1 R_r + a_2$. This modified cutoff function does not fade to zero at short distance but to a small finite value.

Where parameters were not available from the literature, or from Prof. Grimme's website, we have optimized them ourselves against our best S66x8 reference data, using an adaptation of the

20908 | *Phys. Chem. Chem. Phys.*, 2016, **18**, 20905–20925

This journal is © the Owner Societies 2016

Table 2 Basis set extrapolation exponents for various energy components, rounded to four decimal places

	{T,Q}	{Q,5}	{5,6}	
SCF	7.6070	8.7042	9.6897	Karton and Martin[93]
SCF alternate[a]	5.1507	10.3626	12.2568	Schwenke[94]
MP2	2.5313	2.7399	2.8349	Hill *et al.*,[48] Table 8
MP2 alternate[a]	2.5672	2.7028	2.7771	Ranasinghe & Petersson,[95] eqn (11)
CCSD	3.0840	3.2711	3.1937	Schwenke[94]
CCSD-MP2	2.0926	2.2459	2.3546	Ranasinghe & Petersson,[95] Fig. 6
(T)	2.9988	3.6018	3.2279	Schwenke[94]
(T) alternate[a]	3.3950	3.3723	3.3266	Ranasinghe & Petersson,[95] eqn (12)
MP2-F12	4.3548	5.0723	N/A	{T,Q} Hill *et al.*,[48] Table 9; {Q,5} this work
CCSD-F12b	4.5960	6.0642	N/A	{T,Q} Hill *et al.*,[48] Table 10; {Q,5} this work
(T) post F12	2.8950			{T,Q} Hill *et al.*,[48] Table 11

[a] Given for comparison; not used in the present work.

BOBYQA (Bound Optimization BY Quadratic Approximation) optimization program of Powell.[88]

In addition to these molecular mechanics-like corrections, we have also considered the Vydrov–van Voorhis (VV10) "non-local" (NL) dispersion functional,[89] in which an *a posteriori* correction is obtained from the electron density. The required short-range attenuation parameter, b, used for various DFT-NL calculations were obtained from ref. 90 for the conventional DFT functionals and optimized in our group for the DSD double hybrids: the various values are listed in Table 1 of ref. 91 These calculations were carried out using its implementation in ORCA.

The values for DSD-PBEP86-NL and B2GP-PLYP-NL given there differ slightly from those obtained earlier[16] from calculations uncorrected for basis set superposition error; even with the def2-QZVP basis set, the basis set superposition error in a double hybrid is significant enough that this makes a difference for b of as much as one unit.[91]

Symmetry-adapted perturbation theory calculations were carried out using the implementation (ref. 39 and references therein) in a prerelease version of PSI 4.[92]

For the purposes of basis set extrapolation, we employed a two-point expression of the form $E(L) = E_\infty + [E(L) - E(L-1)] / \left[\left(\frac{L}{L-1} \right)^\alpha - 1 \right]$, in which α is taken from Table 2. We wish to point out that all of the various expressions for two-point extrapolation are mathematically equivalent (see, *e.g.*, ref. 93), and have merely converted them to a single form for convenience. Extrapolations of SCF and correlation energies were always performed separately; in the F12 calculations, the SCF component was taken from the largest basis set calculation.

The cc-pV{Q,5}Z-F12 extrapolation exponents in the present work were obtained by following, to the letter, the optimization procedure for the cc-pV{T,Q}Z-F12 exponents detailed in ref. 48.

Calibration of the reference method

Choice of the MP2-F12 reference level

For the smaller, earlier, S22 dataset of noncovalent interactions, a revised set of benchmark data was reported by Marshall, Burns,

and Sherrill (MBS).[12] Aside from total CCSD(T) limit interaction energies given in the paper itself, HLCs (high-level corrections) are given in Table S1 of that paper's ESI, and MP2 limits were extracted as the difference. These correspond to counterpoise-corrected AV{Q,5}Z basis set extrapolation.

Thus, we are able to consider performance for the MP2 basis set limit and for the HLC in isolation.

Our counterpoise-corrected DF-MP2-F12/cc-pVQZ-F12 inter-action energies differ from the MBS estimated MP2 limits by just 0.01 kcal mol^{-1}. This increases to 0.02 kcal mol^{-1} upon cc-pV{T,Q}Z-F12 extrapolation: for the corresponding raw and half-counterpoise values, RMSDs are 0.053 and 0.036 kcal mol^{-1}, respectively.

Calculating DF-MP2-F12/cc-pVTZ-F12 and DF-MP2-F12/cc-pVQZ-F12 energies for the entire S66x8 set proved technically quite feasible, both with and without counterpoise correction. We may conclude that the MP2 component is not the accuracy-limiting factor.

In previous studies[25,27] where comparison with the even larger cc-pV5Z-F12 basis set[27] was possible, it was concluded that half-counterpoise came closest to the basis set limit.

With considerable effort, we were able to obtain DF-MP2-F12/cc-pV5Z-F12 interaction energies for the 1.0r_e slice of S66x8 (which has slightly different geometries than the S66 set – particularly for π stacks). The RMS counterpoise correction at that level is just 0.010 kcal mol^{-1}. Between raw and counterpoise cc-pV{Q,5}Z-F12 extrapolated values – which should ideally be identical – the RMS difference drops even further to 0.004 kcal mol^{-1}. (As noted in the Methods section, the extrapolation exponent in Table 2, 5.0723, was obtained in the present work, and the MP2-F12 correlation component was extrapolated in isolation and combined with the largest basis set HF + CABS component. For the smaller cc-pV{T,Q}Z-F12 sequence, the extrapolation exponent 4.3548 was taken from ref. 48, *cf.* Table 2.)

Error statistics for smaller basis sets can be found in Table 3. The counterpoise-corrected {T,Q}-F12 values deviate from the corresponding {Q,5}-F12 limits by just 0.004 kcal mol^{-1} RMS; for half-counterpoise, this increases to 0.013 kcal mol^{-1} relative to counterpoise {Q,5}-F12, or 0.014 kcal mol^{-1} relative to half-counterpoise {Q,5}-F12 limits. If we were to dispense with extrapolation entirely, half-counterpoise cc-pVQZ-F12 appears

Table 3 RMSD (kcal mol⁻¹) for the MP2-F12 limits of the 1.0r_e slice of S66x8, relative to cc-pV{Q,5}Z-F12 results

	cc-pVTZ-F12	cc-pVQZ-F12	cc-pV5Z-F12	cc-pV{T,Q}Z-F12	cc-pV{Q,5}Z-F12	MP2/AV{T,Q}Z
relative to V{Q,5}Z-F12 raw						
Raw	0.073	0.035	0.009	0.029	REF	
CP	0.050	0.013	0.004	0.006	0.004	0.015
Half	0.017	0.013	0.004	0.016	0.002	
relative to V{Q,5}Z-F12 CP						
Raw	0.070	0.032	0.006	0.026	0.004	
CP	0.053	0.015	0.005	0.004	REF	0.017
Half	0.014	0.010	0.001	0.013	0.002	
relative to V{Q,5}Z-F12 half						
Raw	0.071	0.033	0.007	0.027	0.002	
CP	0.051	0.014	0.004	0.004	0.002	0.016
Half	0.015	0.011	0.003	0.014	REF	

to have a slight edge over full counterpoise, and a definite one over the raw values: in fact, half-counterpoise cc-pVTZ-F12 is found to be preferred over raw cc-pVQZ-F12.

We finally chose full-counterpoise MP2-F12/cc-pV{T,Q}Z-F12 extrapolation as the MP2 component for our benchmark data. Based on the statistics given in Table 3, we conservatively estimate the accuracy of our MP2 limits to be better than 0.01 kcal mol⁻¹.

For comparison, the conventional, counterpoise-corrected MP2/aug-cc-pV{T,Q}Z values used by the Hobza group as the MP2 component of the S66x8 benchmark data in the Benchmark Energy and Geometry Database (www.begdb.com)[14] were recalculated in the present work. They differ from our best reference values by 0.017 kcal mol⁻¹ RMS.

Choice of the high-level correction, i.e., CCSD(T)-MP2 contribution

The S22 dataset as a model. We shall first revisit the S22 set. For some of the larger systems, CCSD(T)-F12b/cc-pVTZ-F12 turned out to be unfeasible in practice: this statement applies to both structures of the adenine···thymine base pair (Watson–Crick and stacked), both structures of indole···benzene (parallel and T-shaped), phenol dimer, and 2-pyridoxine···2-amino-pyridine. We were unable to obtain a counterpoise correction for the stacked uracil dimer, but the uncorrected interaction energy ran to completion, taking more than a week on 32 CPUs.

The crucial factor affecting performance will be the choice of approximation to the (T) connected triple excitations (see Methods section). RMSDs for the HLCs of the S22 set are presented in Table 4.

For the subset, we find that HLC(Ts)/cc-pVTZ-F12 has an RMSD of less than 0.02 kcal mol⁻¹ from the MBS reference data. With the said basis set, there is little to choose between HLC(Ts), HLC(Tb$_{sc}$), and HLC(T*$_{sc}$) – or the non-size-consistent variant HLC(T*), for that matter – as the difference between the RMSDs is less than the presumed uncertainty in the reference data.

Counterpoise correction on the HLC appears to be unhelpful, which is useful considering its computational cost for larger systems. (Counterpoise calculations typically require disabling symmetry.)

For the smaller cc-pVDZ-F12 basis sets, the raw HLCs are definitely preferred over counterpoise and half-counterpoise. Among the size-consistent options, (Tb$_{sc}$) and (Ts) seem to have an edge over (T*$_{sc}$), with there again being little to choose between (Tb$_{sc}$) and (Ts). In our experience,[27] with cc-pVTZ-F12 and larger basis sets, CCSD-F12b and the more rigorous CCSD(F12*),[96] a.k.a. CCSD-F12c, method yield nearly identical results, but with the cc-pVDZ-F12 basis set, CCSD(F12*) may offer an edge for some applications.[25] For the S22 set, we cannot distinguish between the F12b and (F12*) approaches based on the RMSD for HLC alone. We do note, however, that the CCSD-MP2 parts of (F12*)/cc-pVDZ-F12 are considerably closer (RMSD = 0.019 kcal mol⁻¹) to the available F12b/cc-pVTZ-F12 values than the F12b/cc-pVDZ-F12 counterparts (RMSD = 0.044 kcal mol⁻¹).

For the entire S22 set, conventionally computed HLCs with different basis sets are available from the ESI of ref. 12 and 97. The lowest RMSD from the MBS reference data, 0.04 kcal mol⁻¹, is found for counterpoise-corrected CCSD(T)/aug-cc-pV{D,T}Z.

The S66x8 dataset and the 1.0r_e slice thereof. Let us further consider, with the cc-pVDZ-F12 basis set, the differences between various triples corrections for the entire S66x8 set, using cc-pVDZ-F12. Size-consistency errors in CCSD(T*), i.e., with individual scaling for monomers and dimers, range from −0.12 to +0.20 kcal mol⁻¹, clearly unacceptable for our purposes. The difference between Tb$_{sc}$ and Ts, on the other hand, is just 0.015 kcal mol⁻¹ RMSD, with a maximum of 0.086 kcal mol⁻¹ for system 26, stacked uracil dimer at 0.90r_e. (At the equilibrium geometry, this drops to 0.060 kcal mol⁻¹.) For the same system, the largest difference (−0.054 kcal mol⁻¹) is also seen between the (Tc$_{sc}$) obtained from CCSD(F12*) and the (Tb$_{sc}$) from CCSD-F12b. On average, CCSD(F12*) amplitudes result in triples corrections that are systematically smaller (−0.01 kcal mol⁻¹) than those from CCSD-F12b.

Let us consider the CCSD-MP2 differences with the cc-pVDZ-F12 basis set in isolation. Here we do not have to contend with the different (T) options: our two available choices are CCSD(F12*)-MP2-F12 and CCSD-F12b-MP2-F12. The most significant differences between them are seen for systems with multiple hydrogen

20910 | Phys. Chem. Chem. Phys., 2016, 18, 20905–20925

This journal is © the Owner Societies 2016

Table 4 RMSD (kcal mol^{-1}) for the high-level corrections HLC [(CCSD(T)-F12-MP2-F12)/cc-pVnZ-F12] of a subset of S22, relative to the MBS reference data

		HLC(T*)	HLC(Ts)	HLC(T)	HLC(T*$_{sc}$)	HLC(Tb)	HLC(Tb$_{sc}$)
F12b/cc-pVDZ-F12	Raw	0.049	0.047	0.128	0.044	0.055	0.041
	CP	0.126	0.171	0.244	0.143	0.138	0.158
	Half	0.080	0.103	0.184	0.075	0.090	0.090
(F12*)/cc-pVDZ-F12	Raw	0.053	0.041	0.096	0.063	0.052	0.052
F12b/cc-pVTZ-F12	Raw	0.024	0.017	0.043	0.025	0.018	0.018
	CP	0.051	0.071	0.105	0.054	0.063	0.063
	Half	0.031	0.038	0.073	0.022	0.030	0.030

bonds, such as 17 (uracil dimer Watson–Crick), 20 (acetic acid dimer), 21 (acetamide dimer), 22 (acetic acid-uracil), and 23 (acetamide-uracil), for each of which the difference exceeds 0.100 kcal mol^{-1} at equilibrium or compressed geometries. As expected, these differences are greatly reduced for stretched geometries and effectively dwindle to nothing at $2.0r_e$.

(F12*)-F12b differences are smaller, but still some what significant, for π stacks and mixed-influence complexes, but effectively negligible for London complexes.

Which is more correct? At great computational expense and following multiple failures due to Linux kernel tuning issues, we were able to perform CCSD(T)-F12b/cc-pVTZ-F12 calculations for a subset of 58 out of 66 systems at the $1.0r_e$ geometries. The subset consists of all systems except the London complexes 35 and 37–43. The CCSD-MP2 differences in the dissociation energies, obtained as a by-product, should be quite close to the basis set limit. The [CCSD(F12*)-MP2-F12]/cc-pVDZ-F12 agrees with those to 0.013 kcal mol^{-1} RMS (Table 5), compared to 0.040 kcal mol^{-1} for [CCSD-F12b-MP2-F12]/cc-pVDZ-F12. We have hence decided to err on the side of rigor, and to favor CCSD(F12*) over CCSD-F12b, as we have at present no realistic prospect of carrying out CCSD-F12b/cc-pVTZ-F12 calculations for the entire S66x8 dataset.

Performance of different (T) scaling procedures for the HLCs of the 58-system subset has been compared in Table 5. First, we note that they all yield very similar values for the cc-pVTZ-F12 basis set: HLC(Tb$_{sc}$) differs from HLC(Ts) by less than 0.01 kcal mol^{-1} RMS, and by just 0.013 kcal mol^{-1} from HLC(T*$_{sc}$). As generally HLC(Ts) < HLC(Tb$_{sc}$) < HLC(T*$_{sc}$), we have somewhat arbitrarily selected the middle values HLC(Tb$_{sc}$)/cc-pVTZ-F12 for comparison, but another choice would not have led to qualitatively different conclusions.

Second, HLC(Tb$_{sc}$)/cc-pVDZ-F12, HLC(Tc$_{sc}$)/cc-pVDZ-F12, and (Ts) from (F12*)/cc-pVDZ-F12 or F12b/cc-pVDZ-F12 all agree with those values to 0.025–0.042 kcal mol^{-1} RMS, with a possible slight advantage for (F12*)/cc-pVDZ-F12 over F12b/cc-pVDZ-F12. The RMSDs of HLC(Ts)(F12*)/cc-pVDZ-F12 and HLC(Tc$_{sc}$)(F12*)/cc-pVDZ-F12 however are essentially identical, hence no meaningful choice between them can be made from the numbers alone. On the other hand, while (Ts) contains a single empirical parameter (the 'one size fits all' scaling factor), (Tb$_{sc}$) and (Tc$_{sc}$) contain none at all and instead elicit everything from *ab initio* calculations for the actual system at hand. For want of a realistic option to use larger basis sets, we therefore decided on HLC(Tc$_{sc}$)/cc-pVDZ-F12, *i.e.*, with the triples scaled by the E_{corr}[CCSD(F12*)]/E_{corr}[CCSD] ratio, as our final choice for the

Table 5 RMS differences (kcal mol^{-1}) between various high-level corrections with the cc-pVDZ-F12 and cc-pVTZ-F12 basis sets for a 58-system subset of the $1.0r_e$ slice

	HLC(T*)	HLC(T)	HLC(Tb$_{sc}$)	HLC(Ts)	HLC(T*$_{sc}$)
relative to HLC(Tb$_{sc}$)/cc-pVTZ-F12					
F12b/cc-pVTZ-F12	0.021	0.052	REF	0.009	0.013
(F12*)/VDZ-F12	0.045	0.116	0.031	0.025	0.042
F12b/cc-pVDZ-F12	0.042	0.136	0.027	0.036	0.030
relative to HLC(Ts)/cc-pVTZ-F12					
F12b/cc-pVTZ-F12	0.021	0.043	0.009	REF	0.022
(F12*)/VDZ-F12	0.046	0.108	0.036	0.025	0.050
F12b/cc-pVDZ-F12	0.039	0.127	0.026	0.030	0.036
relative to HLC(T*$_{sc}$)/cc-pVTZ-F12					
F12b/cc-pVTZ-F12	0.027	0.065	0.013	0.022	REF
(F12*)/VDZ-F12	0.048	0.129	0.028	0.032	0.034
F12b/cc-pVDZ-F12	0.050	0.149	0.034	0.046	0.026
CCSD-MP2 relative to cc-pVTZ-F12					
F12b/cc-pVTZ-F12	REF				
(F12*)/VDZ-F12	0.013				
F12b/cc-pVDZ-F12	0.040				

reference data. For the 58-system subset, the HLC(Tc$_{sc}$)/cc-pVDZ-F12 combination agrees to 0.031 kcal mol^{-1} RMS with the cc-pVTZ-F12 data, compared to 0.09 kcal mol^{-1} for the counterpoised conventional [CCSD(T)-MP2]/aug-cc-pVDZ HLCs used in the original S66x8 paper, which we reconstructed by recalculating their counterpoised MP2/aug-cc-pV{T,Q}Z components and subtracting from the total S66x8 values.

Counterpoise corrections for lower-level methods

We then are faced with not only the choice of basis set for the lower-level methods, but also the choice of counterpoise correction. It is fairly well-known (*e.g.*, ref. 98) that, for noncovalent interactions, uncorrected dissociation energies approach the basis set limit from above, and counterpoise-corrected ones from below: the half–half counterpoise method, *i.e.*, the average of raw and counterpoise interaction energies, then immediately suggests itself. In ref. 99 it was shown that half-counterpoise generally comes closest to the basis set limit for orbital-based wavefunction *ab initio* calculations. In ref. 26 we showed that this is also generally the case for explicitly correlated methods, except perhaps for large basis sets like cc-pVQZ-F12 and especially cc-pV5Z-F12, where full counterpoise may be more appropriate but the counterpoise corrections in any case become insignificant.

At the HF level, things are rather different. For def2-TZVPP, half-counterpoise appears to have an edge over full counterpoise, but for all larger basis sets full counterpoise "carries the day", with an RMSD as small as 0.005 kcal mol^{-1} for the haVQZ basis set, and 0.013 kcal mol^{-1} for def2-QZVP (Table 6). It hardly matters whether one uses the CABS-corrected HF/cc-pVQZ-F12 or the orbital HF/haV5Z as references: the counterpoise-corrected values for both differ by no more than 0.002 kcal mol^{-1} RMS.

As can be seen in Table 6, HF/def2-QZVP with full counterpoise is quite close to the basis set limit, HF/haVQZ even closer.

What about DFT functionals below rung five? We considered the example of PBE0. Somewhat arbitrarily, we chose haV5Z with full counterpoise correction as the reference: the difference with half-counterpoise in the same basis set amounts to just 0.005 kcal mol^{-1} RMSD (Table 7). For essentially all basis sets considered, full counterpoise is clearly the best of the three options, except that for def2-QZVPD' the gap with half-counterpoise is quite narrow. At any rate, the RMSD of 0.02 kcal mol^{-1} for

def2-QZVP is considered small enough that we can use it for benchmark purposes.

Summing up: for Hartree–Fock and DFT functionals, we will use full counterpoise and a basis of def2-QZVP or better quality.

For MP2, it appears even haVQZ is not adequate to reach the basis set limit, but haV{T,Q}Z extrapolation with full counterpoise does succeed. Half-counterpoise haV5Z comes reasonably close without extrapolation, as does haV{Q,5}Z without counterpoise. In contrast, with the explicitly correlated approach, even MP2-F12/cc-pVTZ-F12 is already within 0.01 kcal mol^{-1} RMS if half-counterpoise is applied (Table 8). At any rate, as reported by Burns *et al.*[99] for conventional correlated calculations and our group[26] for explicitly correlated ones, half-counterpoise is unambiguously preferred.

This finally leaves the double hybrids, where one might expect behavior to be intermediate between MP2 and PBE0. For basis sets def2-QZVP and larger, we can expect the Kohn–Sham part to be converged, which leaves the MP2-like component as the dominant factor in basis set convergence for double hybrids.

Based on the results given in Table 9, we have selected half-counterpoise with the haVQZ basis set as our basis set of choice, with def2-QZVP with half-counterpoise as a fallback. With smaller Weigend–Ahlrichs[41] basis sets, half-counterpoise is again unequivocally preferred, justifying the design decisions taken in ref. 79, 80 and 84.

Results and discussion

Wavefunction *ab initio* results

Since so much work on weak interactions has historically focused on hydrogen bonds (and, to a lesser extent, London dispersion), it is received wisdom in much of the quantum chemical community that MP2 is a "high-level *ab initio*" treatment for noncovalent interactions. In fact, for the S66x8 dataset with the cc-pVQZ-F12 basis set (half counterpoise), the RMSD is a somewhat disappointing 0.69 kcal mol^{-1} (Table 10). Some things become clearer if we break the results down by categories: hydrogen bonds (systems 1–23), π stacks (systems 24–33), London dispersion complexes (systems 34–46), and mixed-influence (systems 47–66). We then see that MP2 has an excellent RMSD = 0.18 kcal mol^{-1} for hydrogen bonds, a tolerable 0.40 kcal mol^{-1} for

Table 6 RMSD (kcal mol^{-1}) for the Hartree–Fock components of the S66x8 interaction energies as calculated with various basis sets

	w.r.t. HF+CABS/cc-pVQZ-F12 CP			w.r.t. HF/haV5Z CP		
	CP	Raw	Half	CP	Raw	Half
haVQZ	0.005	0.026	0.012	0.005	0.026	0.012
haVTZ	0.028	0.110	0.051	0.028	0.110	0.051
def2-QZVP	0.013	0.063	0.031	0.014	0.064	0.031
haV5Z	0.002	0.008	0.004	REF	0.008	0.004
def2-TZVPP	0.046	0.229	0.012	0.046	0.229	0.011
def2-TZVP	0.110	0.298	0.132	0.110	0.298	0.132
VQZ-F12+CABS	REF	0.008	0.004	0.002	0.008	0.004

20912 | *Phys. Chem. Chem. Phys.*, 2016, **18**, 20905–20925

This journal is © the Owner Societies 2016

Table 7 RMSD (kcal mol^{-1}) for the interaction energies of S66x8 set calculated with PBE0 using various basis sets relative to counterpoise corrected PBE0/haV5Z

Counterpoise	CP	Raw	Half
haV5Z	REF	0.009	0.005
haVQZ	0.005	0.046	0.151
haVTZ	0.027	0.093	0.046
def2-QZVP	0.020	0.105	0.054
def2-TZVPP	0.069	0.310	0.157
def2-TZVP	0.143	0.392	0.234
def2-QZVPD'	0.010	0.032	0.015
def2-TZVPPD'	0.028	0.086	0.038
def2-TZVPD'	0.074	0.100	0.122
aug'-pc2	0.025	0.109	0.051
aug'-pc3 (partial results)	0.003	0.010	0.005

Table 8 RMSD (kcal mol^{-1}) for the interaction energies of the S66x8 set relative to half-counterpoise corrected MP2-F12/cc-pV{T,Q}Z-F12

Counterpoise	Raw	CP	Half
MP2-F12/cc-pVTZ-F12	0.058	0.045	0.012
MP2-F12/cc-pVQZ-F12	0.024	0.012	0.007
MP2-F12/cc-pV{T,Q}Z-F12	0.018	REF	0.009
MP2/haVTZ	0.461	0.346	0.162
MP2/haVQZ	0.170	0.150	0.058
MP2/haV5Z	0.073	0.079	0.026
MP2/haV{T,Q}Z	0.047	0.018	0.023
MP2/haV{Q,5}Z	0.028	0.011	0.017
MP2/def2-QZVP	0.158	0.289	0.084

London complexes, and an appalling 1.54 kcal mol^{-1} for π stacks. It has been known for some time (e.g., ref. 100 and 101) that π–π interactions at the MP2 level are severely overestimated due to the dispersion component of the 2nd-order energy effectively corresponding to uncoupled Hartree–Fock dispersion (ref. 102; see also ref. 103).

SCS-MP2 mostly remedies the issue for π stacks, at the expense of degraded performance for London complexes and especially hydrogen bonds. SCS(MI)MP2, optimized for weak interactions, yields fairly poor results for London complexes, but very good to excellent results for the rest of S66x8, at the expense of general thermochemistry. The quasi-first principles S2-MP2[56] trades off some of the great performance for hydrogen bonds for better results in the other categories, still yielding unacceptable pi complexes. Similar to a wrinkle in a carpet larger than the room, the error of parametrized MP2 can be moved from one category to another, but never fully removed. *Ad hoc* fitting of SCS-MP2 yielded $c_{2ab} = 0.339$, $c_{2ss} = 1.429$, RMSD = 0.285 kcal mol^{-1}, somewhat better than the similar SCS(MI)MP2.

Moving on to higher-cost methods, third-order corrections E_3 were evaluated in MP3(F12*)/cc-pVDZ-F12 calculations using Turbomole and added in to half-counterpoise MP2-F12/cc-pVQZ-F12 and spin-component-scaled variants thereof. SCS-MP3 in fact is found to perform worse than SCS-MP2. MP2.5 on the other hand,[104] – averaging between MP2 and MP3, which typically err on opposite sides of the true number – yields a rather pleasing RMSD = 0.21 kcal mol^{-1}, with especially outstanding performance for H-bonds and mixed-influence complexes, while π stacks are still acceptable at 0.44 kcal mol^{-1}. *Ad hoc* refitting of c_3 yields a very modest further improvement in RMSD, while additionally refitting c_{2ss} and c_{2ab} is found to be statistically insignificant.

As an aside, Hesselmann proposed[105] the MP2C method, in which the dispersion part was removed from MP2 and replaced by its TDDFT counterpart. Basis set limit extrapolated MP2C values for the S66 set (i.e., just the equilibrium geometry slice of S66x8) have been reported in ref. 106: the RMSD from their reference data was given as 0.13 kcal mol^{-1}.

Turning now to CCSD(F12*), we find that it actually performs worse than MP2-F12. SCS-CCSD(F12*) greatly improves things, and SCS(MI)CCSD(F12*) especially so (Table 11). *Ad hoc* minimization of RMSD with respect to c_{ss} and c_{ab} yields coefficients fairly close to SCS(MI)CCSD(F12*), yet simply scaling the CCSD(F12*) correlation energy by a factor of 1.23 seems to

Table 9 RMSD (kcal mol^{-1}) for the interaction energies of S66x8 set calculated with the DSD-PBEP86-D3BJ method using various basis sets

	Relative to haV5Z(CP)			Relative to haV5Z(half)			Relative to haV5Z(raw)		
	CP	Raw	Half	CP	Raw	Half	CP	Raw	Half
haV{Q,5}Z	0.036	0.030	0.030	0.017	0.036	0.025	0.046	0.068	0.057
haV5Z	REF	0.076	0.038	0.038	0.038	REF	0.076	REF	0.038
haVQZ	0.034	0.138	0.056	0.070	0.101	0.024	0.108	0.065	0.030
haVTZ	0.130	0.322	0.122	0.165	0.286	0.095	0.201	0.251	0.078
def2-QZVPD'	0.075	0.172	0.059	0.112	0.136	0.037	0.149	0.101	0.046
def2-QZVP	0.102	0.163	0.041	0.139	0.128	0.032	0.176	0.095	0.057
def2-TZVPPD'	0.199	0.353	0.123	0.235	0.319	0.106	0.272	0.285	0.102
def2-TZVPP	0.298	0.348	0.102	0.335	0.315	0.106	0.372	0.284	0.123
def2-TZVPD	0.281	0.380	0.157	0.317	0.349	0.155	0.352	0.319	0.161
def2-TZVP	0.401	0.381	0.203	0.436	0.355	0.216	0.472	0.332	0.234

This journal is © the Owner Societies 2016

Phys. Chem. Chem. Phys., 2016, **18**, 20905–20925 | **20913**

Table 10 Error statistics (kcal mol^{-1}) for the S66x8 interaction energies calculated at the half-counterpoise MP2-F12/cc-pVQZ-F12 level and spin-component scaled variants thereof, as well as with raw [MP3-F12-MP2-F12]/cc-pVDZ-F12 terms added

	MP2-F12	SCS-MP2-F12	SCS(MI)MP2-F12	S2-MP2-F12	SCS-MP3-F12	MP2.5	Ad hoc MP2.Xopt
MSD all	0.293	-0.541	-0.178	0.102	-0.694	-0.012	-0.046
H-bonds	-0.051	-0.732	-0.166	-0.246	-0.753	-0.093	-0.096
π stacks	1.119	-0.240	0.049	0.852	-0.680	0.238	0.141
London	0.228	-0.698	-0.475	0.042	-0.868	-0.112	-0.150
Mixed	0.319	-0.371	-0.113	0.168	-0.520	0.021	-0.012
RMSD all	0.688	0.768	0.342	0.573	0.901	0.207	0.196
H-bonds	0.184	0.967	0.222	0.393	0.972	0.122	0.125
π stacks	1.536	0.527	0.233	1.226	0.887	0.442	0.369
London	0.397	0.881	0.615	0.256	1.090	0.188	0.223
Mixed	0.490	0.477	0.237	0.335	0.654	0.108	0.095
c_{SS}	1.000	1/3	1.290	0.750	1/3	1.000	1.000
c_{AB}	1.000	1.200	0.400	1.150	1.200	1.000	1.000
c_{MP3}	0.000	0.000	0.000	0.000	0.250	0.500	0.556

Table 11 S66x8 error statistics (kcal mol^{-1}) for CCSD(F12*) and spin-component-scaled variants thereof, as well as for CCSD(T)(F12*) and CCSD(T*)(F12*)

	SCS(Adhoc) CCSD(F12*)	SCS-CCSD(F12*)	SCS(MI) CCSD(F12*)	Scaled CCSD(F12*)	CCSD(T) (F12*)	CCSD(T*) (F12*)	CCSD (F12*)	CCSD(F12*) -D2[a]
MSD all	0.003	-0.134	-0.052	-0.016	-0.084	-0.007	-0.586	-0.014
H-bonds	0.020	-0.177	-0.026	-0.054	-0.067	0.011	-0.440	-0.085
π stacks	-0.088	-0.207	-0.171	-0.058	-0.144	-0.044	-1.003	-0.119
London	0.032	-0.068	-0.035	0.052	-0.094	-0.038	-0.688	0.130
Mixed	0.012	-0.090	-0.034	0.004	-0.068	0.013	-0.479	0.027
RMSD all	0.09	0.21	0.11	0.12	0.11	0.05	0.79	0.16
H-bonds	0.06	0.28	0.07	0.14	0.08	0.03	0.56	0.18
π stacks	0.13	0.28	0.22	0.12	0.19	0.06	1.29	0.16
London	0.13	0.14	0.12	0.15	0.12	0.05	0.86	0.20
Mixed	0.04	0.10	0.05	0.05	0.09	0.05	0.61	0.07
c_{SS}	1.312	1.130	1.280	1.230	1	1	1	1
c_{AB}	1.115	1.270	1.110	1.230	1	1	1	1
(T)?	no	no	no	no	yes	yes	no	no

Errors relative to CCSD(Tc$_{sc}$)-F12c/cc-pVDZ-F12. cc-pVDZ-F12 basis set throughout. ^{a} s_6 = 0.225.

work nearly as well, as does adding a Grimme D2 dispersion correction with s_6 = 0.225 (see discussion below together with dRPA75).

At the request of a reviewer, we consider the effect of the new data on the intermolecular separations. In the original S66 paper, the intermolecular separations were obtained by quartic interpolation on the {0.90, 0.95, 1.00, 1.05, 1.10}r_e data points in S66x8 for each complex. We have repeated this procedure for both the original S66x8 data obtained from www.begdb.com and for the present revised data in Table 1. The minimum-energy intermolecular separations from both datasets are compared in the master data spreadsheet in the ESI,† while the Cartesian coordinates corresponding to them are also made available in .xyz format in the ESI.†

By and large, the higher level of theory in the present data (particularly for the HLC) does not translate into dramatic geometry changes: the separations change by −0.00074r_e on average (the revised geometries being slightly shorter than the originals), 0.00246r_e mean absolute difference, and 0.00285r_e RMS difference. The largest differences are +0.0066r_e for benzene⋯ethene (system 30) and −0.0063r_e for pyridine⋯ethyne (system 65). Generally speaking, the revised data lead to stretching for the pi stacks and contraction for the hydrogen bonds, with mixed behavior seen for the remaining systems.

How consequential are these geometry differences for the total energy? We evaluated DF-SCS(MI)MP2-F12/cc-pVTZ-F12 energies at both sets of geometries: the RMS difference between the total energies over the S66 systems was found to be just

20914 | *Phys. Chem. Chem. Phys.*, 2016, **18**, 20905–20925

This journal is © the Owner Societies 2016

Table 12 Error statistics (kcal mol^{-1}) for interaction energies of S66x8 set calculated with MP2, HF and various DFT methods

Counterpoise	Half	Half	Half	Half	Half	Half	Half	Half	Full
Method	MP2	B2PLYP	B2GP-PLYP	DSD-PBEP86-noD	DSD-PBEPBE-noD	DSD-PBEB95-noD	DSD-APF	dRPA75	PBE0
Basis set	def2-QZVP	haVQZ	haVQZ	haVQZ	haVQZ	haVQZ	def2-QZVP	haV{Q,5}Z	def2-QZVP
MSD all	0.25	-1.37	-1.00	-0.70	-1.06	-0.80	-1.00	-0.82	-1.56
H-bonds	0.12	-0.77	-0.51	-0.45	-0.78	-0.75	-0.67	-0.60	-0.66
π stacks	-1.09	-2.26	-1.63	-1.06	-1.53	-1.05	-1.49	-1.29	-3.00
London	-0.22	-1.98	-1.52	-1.06	-1.47	-0.98	-1.45	-1.03	-2.34
Mixed	-0.27	-1.24	-0.89	-0.59	-0.87	-0.62	-0.83	-0.69	-1.37
RMSD all	0.68	1.82	1.33	0.93	1.37	1.00	1.28	1.09	2.23
H-bonds	0.24	0.92	0.63	0.57	0.96	0.95	0.81	0.73	0.85
π stacks	1.51	2.81	2.01	1.33	1.93	1.29	1.82	1.68	3.77
London	0.40	2.37	1.81	1.27	1.80	1.16	1.73	1.30	2.86
Mixed	0.46	1.54	1.12	0.74	1.09	0.75	1.02	0.88	1.77
Counterpoise	Full	Full	Full	Full	Full	Full	Full	Full	Full
Method	TPSS0	B3P86	B3LYP	B3PW91	PW6B95	APF	ωB97X-V without NL	M11	MN12SX
Basis set	def2-QZVP	def2-QZVP	def2-QZVP	def2-QZVP	def2-QZVP	def2-QZVP	def2-QZVP	def2-QZVP	def2-QZVP
MSD all	-2.04	-2.27	-2.49	-2.83	-1.25	-2.08	-1.92	0.62	1.14
H-bonds	-1.10	-1.21	-1.35	-1.77	-0.93	-1.12	-1.29	0.61	1.19
π stacks	-3.59	-3.87	-4.35	-4.56	-2.05	-3.64	-3.19	0.84	1.19
London	-2.93	-3.26	-3.45	-3.89	-1.53	-2.98	-2.51	0.69	1.29
Mixed	-1.78	-2.06	-2.26	-2.50	-1.04	-1.84	-1.62	0.48	0.95
RMSD all	2.79	3.00	3.36	3.67	1.63	2.81	2.54	0.75	1.31
H-bonds	1.32	1.41	1.62	2.04	1.16	1.33	1.58	0.73	1.36
π stacks	4.50	4.75	5.46	5.64	2.57	4.54	4.05	0.97	1.40
London	3.61	3.86	4.19	4.69	1.86	3.61	3.07	0.81	1.44
Mixed	2.27	2.52	2.83	3.08	1.30	2.31	2.04	0.57	1.09
Counterpoise	Full	Full	Full	Full	Full	Full	Full	Full	Full
Method	M06	M06-2X	TPSS	M06L	PBE	BP86	BLYP	B97D w/o D	HF
Basis set	def2-QZVP	def2-QZVP	def2-QZVP	def2-QZVP	def2-QZVP	def2-QZVP	def2-QZVP	def2-QZVP	def2-QZVP
MSD all	-0.77	0.29	-2.26	0.69	-1.63	-2.79	-3.12	-3.31	-3.08
H-bonds	-0.72	0.26	-1.31	0.71	-0.74	-1.70	-1.95	-2.41	-2.12
π stacks	-1.22	0.29	-3.86	0.85	-3.10	-4.48	-5.10	-5.13	-5.15
London	-0.59	0.42	-3.12	0.49	-2.33	-3.81	-4.11	-4.18	-3.97
Mixed	-0.73	0.23	-2.01	0.72	-1.47	-2.53	-2.82	-2.87	-2.57
RMSD all	0.97	0.45	3.08	0.80	2.34	3.57	4.10	4.40	4.19
H-bonds	0.83	0.38	1.59	0.79	0.99	1.95	2.33	2.93	2.64
π stacks	1.49	0.55	4.90	0.99	3.97	5.49	6.42	6.67	6.70
London	0.81	0.57	3.89	0.59	2.90	4.52	5.01	5.32	5.00
Mixed	0.87	0.38	2.55	0.84	1.90	3.06	3.50	3.66	3.38

0.004 kcal mol^{-1}. This is immaterial for all but the highest-accuracy work – and then one would wish to optimize monomer geometries at a higher level as well.

Performance of density functional methods

Without dispersion corrections. In Table 12, performance for DFT functionals without dispersion correction is considered. Unsurprisingly, the various uncorrected DFT functionals perform quite poorly. Straight HF sets perhaps the low-water-mark for performance, with RMSD from 2.6 kcal mol^{-1} for H bonds to 6.7 kcal mol^{-1} for π-stack, and 4.19 kcal mol^{-1} overall. PBE and PBE0 actually perform a good deal better than that for hydrogen bonds, but still yield a disappointing 2.3 and 2.2 kcal mol^{-1} overall, respectively, owing primarily to π stacks and London complexes.

For straight MP2 this drops to 0.68 kcal mol^{-1}, which would be a lot better if it weren't for the poor performance for π stack (RMSD = 1.5 kcal mol^{-1}). MP2 actually holds its own quite well for H-bonds (0.24 kcal mol^{-1}) and reasonably well for London and mixed complexes.

Table 13 Error statistics (kcal mol^{-1}) for interaction energies of S66x8 set calculated with D2 dispersion corrected MP2, HF and various DFT methods

Counterpoise	Half	Half	Half	Half	Half	Half	Half	Half
Method	MP2-D2	B2PLYP-D2	B2GP-PLYP-D2	DSD-PBEP86-D2	DSD-PBEPBE-D2	DSD-PBEB95-D2	DSD-APF-D2	dRPA75-D2
Basis set	def2-QZVP	haVQZ	haVQZ	haVQZ	haVQZ	haVQZ	def2-QZVP	haV{Q,5}Z
MSD all	0.32	0.02	0.02	-0.02	0.01	-0.07	-0.06	-0.02
H-bonds	0.56	0.10	0.12	-0.02	-0.12	-0.30	-0.09	-0.10
π stacks	-0.25	-0.10	-0.06	0.00	0.12	0.09	-0.05	-0.06
London	0.50	0.02	-0.06	-0.08	0.06	0.07	-0.12	0.11
Mixed	0.22	0.00	0.01	0.02	0.08	0.03	0.00	0.01
RMSD all	0.61	0.22	0.20	0.15	0.23	0.32	0.23	0.15
H-bonds	0.71	0.19	0.21	0.15	0.23	0.44	0.19	0.18
π stacks	0.66	0.22	0.20	0.20	0.32	0.29	0.33	0.12
London	0.67	0.33	0.24	0.16	0.22	0.25	0.25	0.17
Mixed	0.35	0.16	0.15	0.12	0.18	0.18	0.19	0.06
s_6	-0.16	0.55	0.40	0.27	0.42	0.29	0.37[a]	0.314[a]
Counterpoise	Full	Full	Full	Full	Full	Full	Full	Full
Method	PBE0-D2	TPSS0-D2	B3P86-D2	B3LYP-D2	B3PW91-D2	PW6B95-D2	APF-D2	ωB97X-V without NL, adding D2
Basis set	def2-QZVP	def2-QZVP	def2-QZVP	def2-QZVP	def2-QZVP	def2-QZVP	def2-QZVP	def2-QZVP
MSD all	-0.03	0.12	-0.24	0.18	-0.03	0.02	-0.02	-0.05
H-bonds	0.29	0.25	0.05	0.30	-0.03	-0.14	0.16	-0.13
π stacks	-0.64	-0.25	-0.73	-0.22	-0.24	-0.09	-0.46	-0.30
London	-0.15	0.16	-0.35	0.37	0.11	0.29	-0.03	0.17
Mixed	-0.02	0.13	-0.26	0.11	-0.03	0.09	-0.01	0.04
RMSD all	0.46	0.41	0.56	0.48	0.47	0.34	0.40	0.31
H-bonds	0.47	0.44	0.45	0.41	0.33	0.28	0.39	0.29
π stacks	0.78	0.43	0.86	0.35	0.56	0.24	0.57	0.36
London	0.36	0.48	0.63	0.80	0.69	0.53	0.45	0.42
Mixed	0.24	0.31	0.40	0.30	0.36	0.27	0.26	0.20
s_6	0.60	0.85	0.80	1.05	1.10	0.50	0.81[a]	0.73[a]
Counterpoise	Full	Full	Full	Full	Full	Full	Full	Full
Method	M06-D2	TPSS-D2	M06L-D2	PBE-D2	BP86-D2	BLYP-D2	B97D2	HF-D2
Basis set	def2-QZVP	def2-QZVP	def2-QZVP	def2-QZVP	def2-QZVP	def2-QZVP	def2-QZVP	def2-QZVP
MSD all	-0.14	0.28	0.18	0.28	-0.11	-0.07	-0.13	0.10
H-bonds	-0.32	0.27	0.39	0.44	-0.04	-0.06	-0.44	-0.15
π stacks	-0.24	0.06	0.06	-0.16	-0.35	-0.39	-0.22	-0.24
London	0.32	0.52	-0.24	0.40	0.01	0.25	0.36	0.58
Mixed	-0.17	0.24	0.27	0.22	-0.16	-0.12	-0.05	0.24
RMSD all	0.51	0.52	0.45	0.50	0.54	0.43	0.51	0.60
H-bonds	0.45	0.43	0.48	0.57	0.41	0.25	0.68	0.56
π stacks	0.42	0.43	0.30	0.32	0.66	0.47	0.41	0.71
London	0.80	0.80	0.54	0.66	0.78	0.73	0.54	0.81
Mixed	0.35	0.41	0.42	0.35	0.42	0.27	0.24	0.39
s_6	0.25	1.00	0.20	0.75	1.05	1.20	1.25	1.25

[a] Obtained in the present work by minimization of S66x8 RMSD.

By far the best performer without any dispersion correction is M06-2X, at RMSD = 0.43 kcal mol^{-1}. M06 has over twice that error (0.95 kcal mol^{-1}). At 0.74 and 1.30 kcal mol^{-1}, respectively, M11 and M12 do not offer relief either.

Simple double hybrids perform fairly poorly, RMSD = 1.82 kcal mol^{-1} for B2PLYP and 1.33 kcal mol^{-1} for B2GP-PLYP. The DSD-noD functionals are in the 0.9–1.4 kcal mol^{-1} range, and thus arguably "do not earn their keep", since they are outperformed by straight MP2.

Very recently, Kallay and coworkers proposed[81] the dRPA75 functional, in which the correlation is obtained from a dRPA (direct random phase approximation,[107] a.k.a. drCCD or direct ring coupled cluster[82,108]) with all doubles calculation in a set

of orbitals involving a mixture of 75% Hartree–Fock-like exchange and 25% PBE exchange. Using the haVTZ basis set, RMSD without counterpoise correction is a deceptively low 0.37 kcal mol^{-1}; this rises to 0.77 kcal mol^{-1} for def2-QZVP, 0.71 kcal mol^{-1} for haVQZ, 0.89 kcal mol^{-1} for haV5Z, and 1.09 kcal mol^{-1} at the haV{Q,5}Z extrapolated limit. At the basis set limit, raw and counterpoise-corrected values agree tolerably well, yet one manifestly sees very slow basis set convergence akin to a conventional wavefunction method.

With dispersion corrections. We now consider the simple D2 empirical dispersion. Even this rudimentary correction dramatically improves performance of functionals like PBE, PBE0, and B3LYP; even for straight HF, adding D2 brings down

RMSD to about 0.6 kcal mol^{-1} (Table 13). M06, which was designed to implicitly account for intermediate-range dispersion, still benefits from the long-range D2 correction (RMSD lowered from 0.97 to 0.51 kcal mol^{-1}) (Table 13). The π stacks and/or the London complexes are typically the most problematic subset, but for B97D2 it is actually the hydrogen-bonded complexes. PW6B95-D2 puts in a highly creditable performance, at RMSD = 0.33 kcal mol^{-1}, as does the ωB97X-V functional, with the NL correction deleted and replaced by D2.

Of the simple double hybrids, both B2PLYP-D2 and B2GP-PLYP-D2 exhibit excellent performances (RMSD = 0.22 and 0.20 kcal mol^{-1}, respectively, even including π stack dimers). DSD-PBEP86-D2 yields the best result of all the D2-corrected functionals, at RMSD = 0.15 kcal mol^{-1}.

The most significant improvement is seen for dRPA75. At the half-counterpoise haV{Q,5}Z limit, adding a D2 correction with $s_6 = 0.314$ leads to RMSD = 0.15 kcal mol^{-1}, which changes the performance of dRPA75 from mediocre to best of class. A partial rationale is offered by considering the statistical correlation between (Tb) and the D2 correction: for the entire S66x8 set, $R^2 = 0.92$. This is perhaps not surprising, from an SAPT perspective, in view of the importance of fourth-order (T) in the correction to the dispersion energy. dRPA can, after all, be seen as an approximation to CCSD. By way of further illustration, we considered adding D2 corrections to CCSD(F12*) itself, which leads to $s_6 = 0.225$ and RMSD = 0.156 kcal mol^{-1}, not dissimilar to dRPA75-D2.

Switching from D2 to the more sophisticated D3BJ empirical correction improves statistics for virtually all the GGAs, meta-GGAs, and hybrids. (The two exceptions are straight HF – which could be regarded as a "hybrid" with 100% exact exchange and null correlation – and PW6B95.) For BLYP-D3BJ, for instance, an amazingly low RMSD = 0.23 kcal mol^{-1} is obtained, while B3LYP-D3BJ yields essentially the same performance to within the uncertainty of the reference dataset (Table 14). Several other functionals can attain values around 0.3 kcal mol^{-1}, such as TPSS0-D3BJ and B3PW91-D3BJ.

The APF functional[71] (RMSD = 0.26 kcal mol^{-1} for APF-D3BJ) was designed to be more or less "dispersion-free": specifically, it consists of a linear combination of B3PW91 and PBE0 chosen such that the dissociation curve of Ne_2 (a paradigmatically dispersion-bound system) is as close to the repulsive Hartree–Fock results as possible. D3BJ parameters were fitted in this work: noteworthy is the large positive s_8 coefficient. The latter corresponds to an additional correction in the medium-range region. For perspective, we also fitted D3BJ parameters for straight MP2, and found a large negative $s_8 = -3.35$, corresponding to RMSD = 0.31 kcal mol^{-1}. For additional perspective, we fitted D3BJ parameters for dRPA75, and found that RMSD dropped to 0.10 kcal mol^{-1} with both a_1 and s_8 constrained to zero. No statistically significant change was seen when relaxing the $s_8 = 0$ constraint. In other words, while dRPA75 does not recover all long-range dispersion, it appears to recover the intermediate range.

Exploring this point a little further, we considered fitting M06-D3BJ. No stable fit could be obtained unless the constraints $a_1 = s_8 = 0$ were applied, in which case RMSD dropped to 0.40 kcal mol^{-1}. It thus appears that the main benefit of M06 over conventional hybrid GGAs is likewise in the intermediate-distance region (*vide supra*).

What about the double hybrids? While for B2PLYP-D3BJ, $s_8 = 0.91$ and thus quite nontrivial, for B2GP-PLYP-D3BJ $s_8 = 0.26$ and $a_1 = 0.00$, corresponding to RMSD = 0.23 kcal mol^{-1}. For DSD-PBEP86-D3BJ, on the other hand, a stable fit required setting $s_8 = a_1 = 0.00$: this pattern repeats itself across all the DSD double hybrids. Effectively, this means that, for weak interactions, (a) the principal benefit of double hybrids and RPA correlation alike is correction in the intermediate distance region; (b) since straight MP2 overcorrects in that region, this needs to be tempered by either including higher-order correlation (as in dRPA75 or MP2.5) or by throttling the MP2 correlation term (as happens in double hybrids). We attempted replacing the dRPA correlation term in dRPA75 by an MP2-like term, and found qualitatively the same behavior as for ordinary MP2.

Overall, for the double hybrids, improvements from using D3BJ instead of D2 are marginal at best, while DSD-PBEP86-D2 even outperforms DSD-PBEP86-D3BJ. We note that, aside from the s_8 term being effectively absent (or not fittable at a statistically significant level), a large part of dispersion is already covered by the MP2-like terms.

We optimized a new DSD double hybrid based on the APF "dispersion-free" hybrid, with the idea that this would eliminate some double-counting. It yields a respectable RMSD = 0.23 kcal mol^{-1}, which is however no improvement over DSD-PBEP86-NL.

dRPA75-D3BJ, with $s_6 = 0.3754$, $a_2 = 4.5048$, $a_1 = s_8 = 0$, improves further (to 0.10 kcal mol^{-1}) on the already outstanding performance of dRPA75-D2.

In a very recent benchmark study on the conformer energies of the proteinogenic amino acids, we noted excellent performance of the uncorrected dRPA75/def2-QZVP method, RMSD = 0.21 kcal mol^{-1} (Boltzmann-weighted, $T_B = 1000$ K) or 0.37 kcal mol^{-1} (unit weights). We re-evaluated these statistics using dRPA75-D2/def2-QZVP and dRPA75-D3BJ/def2-QZVP. With the D2 dispersion correction, statistics for the conformer set actually were degraded to 0.42 (Boltzmann) and 0.70 (unit weights) kcal mol^{-1}. The D3BJ correction, on the contrary, improved the statistics to 0.14 (Boltzmann) and 0.32 (unit weights) kcal mol^{-1}, comparable to the best performers in that paper. It was previously shown (*e.g.*, see ref. 109 and 110 for alkanes) that midrange dispersion interactions are very important in conformer equilibria, and that D2 is often more of a hindrance than a help for these properties owing to the form of the cutoff function; D3BJ, on the other hand, does not exhibit this problem.[110] As we have shown earlier in the manuscript that unassisted dRPA75 already works well in the medium distance range, adding D2 for conformer equilibria amounts to "fixing what ain't broke".

Concerning range-separated double hybrids, we note that Head-Gordon's recent "survival of the fittest/most transferable" ωB97X-V (0.23 kcal mol^{-1}), which involves NL as its dispersion component, is actually slightly improved by replacing NL with a

Paper

Table 14 Error statistics (kcal mol^{-1}) for interaction energies of S66x8 set calculated with D3BJ dispersion corrected MP2, HF and various DFT methods

Counterpoise	Half	Half	Half	Half	Half	Half	Half	Half
Method	MP2-D3BJ	B2PLYP-D3BJ	B2GP-PLYP-D3BJ	DSD-PBEP86-D3BJ	DSD-PBEPBE-D3BJ	DSD-PBEB95-D3BJ	DSD-APF-D3BJ	dRPA75-D3BJ
Basis set	def2-QZVP	haVQZ	haVQZ	haVQZ	haVQZ	haVQZ	def2-QZVP	haV{Q,5}Z
MSD all	0.03	-0.09	-0.11	0.09	0.05	-0.01	-0.05	0.01
H-bonds	0.20	-0.02	-0.01	0.04	-0.13	-0.29	-0.09	-0.02
π stacks	-0.17	-0.03	-0.08	0.27	0.36	0.32	0.08	-0.04
London	-0.03	-0.21	-0.31	0.02	0.05	0.12	-0.17	0.05
Mixed	-0.03	-0.10	-0.12	0.12	0.11	0.08	0.00	0.03
RMSD all	0.31	0.19	0.22	0.20	0.25	0.33	0.21	0.10
H-bonds	0.34	0.13	0.13	0.12	0.23	0.43	0.18	0.09
π stacks	0.45	0.19	0.16	0.38	0.47	0.43	0.33	0.15
London	0.23	0.28	0.39	0.10	0.15	0.19	0.23	0.09
Mixed	0.22	0.17	0.18	0.17	0.17	0.18	0.16	0.07
s_6	1.049*	0.640	0.560	0.480	0.780	0.580	0.574*	0.375*
s_8	-3.351*	0.915	0.260	0.000	0.000	0.000	0.000	0.000
a_1	-0.478*	0.307	0.000	0.000	0.000	0.000	0.000	0.000
a_2	9.254*	5.057	6.333	5.600	6.100	6.200	5.623*	4.505*
Counterpoise	Full	Full	Full	Full	Full	Full	Full	Full
Method	PBE0-D3BJ	TPSS0-D3BJ	B3LYP-D3BJ	B3PW91-D3BJ	PW6B95-D3BJ	APF-D3BJ	ωB97X-V without NL, adding D3BJ	CAM-B3LYP-D3BJ
Basis set	def2-QZVP	def2-QZVP	def2-QZVP	def2-QZVP	def2-QZVP	def2-QZVP	def2-QZVP	def2-QZVP
MSD all	0.12	0.01	0.05	-0.04	-0.10	0.02	0.01	-0.075
H-bonds	0.30	0.12	0.16	-0.14	-0.31	0.10	-0.03	-0.409
π stacks	-0.13	-0.10	-0.01	0.26	-0.05	0.01	-0.12	0.263
London	0.02	-0.13	-0.03	-0.12	0.12	-0.09	0.09	0.101
Mixed	0.11	0.03	-0.01	-0.04	-0.03	0.02	0.09	0.025
RMSD all	0.35	0.30	0.20	0.31	0.34	0.26	0.20	0.429
H-bonds	0.46	0.36	0.28	0.35	0.45	0.33	0.18	0.569
π stacks	0.39	0.28	0.19	0.44	0.35	0.28	0.29	0.551
London	0.25	0.32	0.13	0.22	0.25	0.23	0.16	0.250
Mixed	0.21	0.20	0.13	0.20	0.23	0.18	0.18	0.204
s_6	1.000	1.000	1.000	1.000	1.000	1.000*	1.000*	1.000
s_8	1.218	1.258	1.989	2.852	0.726	1.776*	0.126*	2.067
a_1	0.415	0.377	0.398	0.431	0.208	0.341*	0.211*	0.371
a_2	4.859	4.587	4.421	4.469	6.375	4.995*	4.350*	5.474
Counterpoise	Full	Full	Full	Full	Full	Full	Full	Full
Method	ωB97XD3	LC-ωPBE-D3BJ	TPSS-D3BJ	PBE-D3BJ	BP86-D3BJ	BLYP-D3BJ	B97D3	HF-D3BJ
Basis set	def2-QZVP	def2-QZVP	def2-QZVP	def2-QZVP	def2-QZVP	def2-QZVP	def2-QZVP	def2-QZVP
MSD all	-0.08	0.03	-0.06	0.09	0.23	-0.11	0.00	0.33
H-bonds	0.02	0.18	-0.03	0.28	0.11	-0.14	-0.28	0.54
π stacks	0.02	-0.14	-0.10	-0.22	0.67	0.05	0.24	-0.22
London	-0.41	0.02	-0.10	0.06	0.23	-0.08	0.20	0.26
Mixed	-0.02	-0.04	-0.06	0.05	0.14	-0.16	0.06	0.41
RMSD all	0.32	0.25	0.34	0.36	0.58	0.23	0.37	0.63
H-bonds	0.16	0.30	0.29	0.39	0.48	0.26	0.47	0.80
π stacks	0.34	0.26	0.46	0.55	1.07	0.25	0.41	0.59
London	0.57	0.19	0.42	0.32	0.48	0.17	0.32	0.42
Mixed	0.17	0.21	0.26	0.21	0.37	0.23	0.24	0.53
s_6		1.000	1.000	1.000	1.000	1.000	1.000	1.000
s_8		1.854	1.944	0.788	3.282	2.700	2.261	0.917
a_1		0.392	0.454	0.429	0.395	0.430	0.555	0.339
a_2		5.090	4.475	4.441	4.852	4.236	3.230	2.883

D3BJ parameters taken from http://www.thch.uni-bonn.de/tc/downloads/DFT-D3/functionalsbj.html except where indicated by (*), which were optimized in this work, and for DSD double hybrids, taken from ref. 80.

custom-fitted D3BJ. This may prove useful for codes in which no implementation of NL is available. While CAM-B3LYP-D3BJ does considerably worse than B3LYP-D3BJ, LC-ωPBE-D3BJ well outperforms both PBE-D3BJ and PBE0-D3BJ.

Table 15   Error statistics (kcal mol^{-1}) for interaction energies of S66x8 set calculated with MP2, HF and various DFT methods considering NL correction

Counterpoise	Half	Half	Half	Half	Half	Half	Half
Method	B2PLYP-NL	B2GP-PLYP-NL	DSD-PBEP86-NL	DSD-PBEPBE-NL	DSD-PBEB95-NL	DSD-APF-NL	PBE0-NL
Basis set	haVQZ	haVQZ	haVQZ	haVQZ	haVQZ	def2-QZVP	def2-QZVP
MSD all	-0.01	0.01	0.02	-0.01	-0.06	-0.03	0.03
H-bonds	0.11	0.13	0.00	-0.11	-0.29	-0.06	0.37
π stacks	-0.01	0.04	0.13	0.20	0.18	0.12	-0.39
London	-0.12	-0.12	-0.05	-0.03	0.06	-0.11	-0.18
Mixed	-0.09	-0.04	0.03	0.02	0.01	-0.01	-0.03
RMSD all	0.18	0.17	0.12	0.18	0.27	0.16	0.45
H-bonds	0.21	0.22	0.10	0.19	0.41	0.14	0.59
π stacks	0.15	0.12	0.19	0.26	0.23	0.22	0.56
London	0.19	0.19	0.15	0.19	0.14	0.20	0.32
Mixed	0.15	0.11	0.08	0.10	0.12	0.11	0.23
NLb[a]	7.8	9.9	12.8	9.6	12.5	10.2	6.9
Counterpoise	Full	Full	Full	Full	Full	Full	Full
Method	TPSS0-NL	B3P86-NL	B3LYP-NL	B3PW91-NL	PW6B95-NL	APF-NL	ωB97X-V
Basis set	def2-QZVP	def2-QZVP	def2-QZVP	def2-QZVP	def2-QZVP	def2-QZVP	def2-QZVP
MSD all	-0.01	-0.11	-0.08	-0.27	-0.10	0.02	-0.08
H-bonds	0.24	0.22	0.26	-0.05	-0.20	0.27	-0.08
π stacks	-0.23	-0.32	-0.39	-0.35	-0.16	-0.19	-0.16
London	-0.22	-0.35	-0.23	-0.49	0.06	-0.15	-0.03
Mixed	-0.07	-0.24	-0.22	-0.35	-0.07	-0.05	-0.07
RMSD all	0.40	0.48	0.42	0.47	0.26	0.37	0.23
H-bonds	0.54	0.65	0.46	0.47	0.31	0.56	0.20
π stacks	0.33	0.36	0.56	0.41	0.30	0.24	0.37
London	0.35	0.40	0.31	0.57	0.19	0.22	0.18
Mixed	0.24	0.33	0.33	0.43	0.22	0.20	0.19
NLb[a]	5.5	5.3	4.8	4.5	9.0	5.4	6.0
NLc							0.01
Counterpoise	Full	Full	Full	Full	Full	Full	Full
Method	M06-NL	TPSS-NL	PBE-NL	BP86-NL	BLYP-NL	B97D-NL	HF-NL
Basis set	def2-QZVP	def2-QZVP	def2-QZVP	def2-QZVP	def2-QZVP	def2-QZVP	def2-QZVP
MSD all	-0.16	0.01	0.12	-0.10	-0.14	-0.07	-0.14
H-bonds	-0.33	0.22	0.41	0.12	0.09	-0.18	-0.17
π stacks	-0.22	-0.13	-0.24	-0.10	-0.28	0.16	-0.20
London	0.28	-0.09	0.06	-0.22	-0.18	0.08	-0.11
Mixed	-0.21	-0.09	0.01	-0.27	-0.31	-0.14	-0.08
RMSD all	0.44	0.34	0.41	0.44	0.33	0.33	0.56
H-bonds	0.44	0.45	0.55	0.58	0.26	0.32	0.51
π stacks	0.35	0.29	0.47	0.32	0.38	0.36	0.91
London	0.59	0.29	0.27	0.31	0.24	0.36	0.46
Mixed	0.34	0.24	0.22	0.35	0.40	0.31	0.42
NLb[a]	14.4	5.0	6.4	4.4	4.0	3.6	3.9

[a] NLb parameters obtained in ref. 91 and taken from Table 1. Any remaining NLb parameters taken from ref. 90, except ωB97X-V from the original ref. 76.

We now turn to the Vydrov–Van Voorhis[89] "nonlocal" (NL) dispersion correction. This correction effectively only has a single adjustable parameter NLb, which governs short-range attenuation. There are no atomic parameters, as this information is extracted *a posteriori* from the calculated electron density.

For many functionals such as PBE, PBE0, TPSS0, BLYP, B3LYP, and B3PW91, NL actually performs worse than D3BJ, while for TPSS the two appear to be of the same quality. For

BP86, B97D, HF, and PW6B95, it clearly is superior to D3BJ, besides having the obvious advantage that no atomic parameters are required at all (Table 15).

Among the simple double hybrids, NL does marginally better than D2 and D3BJ for B2GP-PLYP (RMSD = 0.17 kcal mol^{-1}).

Yu[16] proposed adding the correction to spin-component scaled double hybrids. His optimization procedure neglects the quite considerable BSSE in the S66 series: in the framework of our recent

study on amino acid conformers[91] we reoptimized his proposed restriction parameters: these are the ones used in the present work.

In relative terms, it may well be the DSD double hybrids that benefit most. For DSD-PBEP86-NL, RMSD drops to just 0.12 kcal mol^{-1}, coupled with the excellent performance of DSD-PBEP86 for thermochemical and kinetic properties[79,80] as well as for vibrational frequencies.[111] But also for DSD-PBEPBE-NL (0.18 kcal mol^{-1}), DSD-APF-NL (0.16 kcal mol^{-1}), and to a lesser extent for DSD-PBEhB95-NL (0.27 kcal mol^{-1}) significant improvements over the corresponding D3BJ functionals were seen. The π-stacking complexes benefit most, their RMS errors typically being about halved.

The DSD-APF-NL functional, which yielded the second best performance, was actually created by simply applying 0.411*DSD-PBE+(1-0.411)*DSD-BPW91, each with parameters taken from ref. 80

Functionals of the form DSD-XC-NL not only appear to have excellent performance, but they come with two additional advantages: (1) there is no need for an elaborate set of atomic dispersion parameters; (2) the method is no longer open to the criticism that it involves "adulterating" an electronic structure method with Lennard-Jones type corrections.

The advantages of NL for double hybrids are not evident if only equilibrium values (i.e., S66) are considered: it is at compressed geometries that they yield their greatest benefits.

The original D3BJ parameters for the DSD functionals were optimized using half-counterpoise with the relatively small def2-TZVP basis set, mostly from the S22 and Grubbs catalyst benchmarks. We considered performance when refitting against the present S66x8 data. For DSD-PBEP86-D3BJrefit, we obtain RMSD = 0.158 kcal mol^{-1} for $s_6 = 0.468$ and $a_2 = 5.857$, which closes some of the gap with DSD-PBEP86-NL but not all of it. For DSD-PBEPBE-D3BJ, RMSD = 0.193 kcal mol^{-1} is statistically indistinguishable from the DSD-PBEPBE-NL number; the revised parameters are $s_6 = 0.518$ and $a_2 = 4.846$. For DSD-PBEhB95-D3BJ, refitting yields $s_6 = 0.263$ and a somewhat anomalous $a_2 = 3.360$, with RMSD = 0.204 kcal mol^{-1} actually better than DSD-PBEhB95-NL.

How does the substitution of NL for D3BJ affect performance for other test sets, such as barrier heights, atomization energies, and the like? We considered the six training sets used in parametrizing the original functionals. The results can briefly be summarized as implying that D3BJ and NL yield results of similar quality considering the residual uncertainty in the reference values. It therefore appears to pass the "above all, do no harm" test.

On the other hand, D3BJ is available in several additional codes beyond ORCA, and derivatives are trivial to implement (unlike for NL).

SAPT results and a proposed new noncovalent character index

From a SAPT perspective, the SCF component of the interaction energy can be decomposed as follows:[39,112]

$$IE_{SCF} = E_{elst}^{(10)} + E_{exch}^{(10)} + E_{ind}^{(20)} + E_{exch-ind}^{(20)} + E_{ind}^{(30)} + E_{exch-ind}^{(30)} + \delta SCF_3 \tag{4}$$

$$IE_{SCF} = E_{elst}^{(10)} + E_{exch}^{(10)} + E_{ind}^{(20)} + E_{exch-ind}^{(20)} + \delta SCF_2 \tag{5}$$

where in this and the following equations, blue terms are attractive, red terms are repulsive, black terms can go either way, the two superscripts indicate order of inter- and intra-molecular perturbation theory, respectively, and the subscript "elst", "ind", "exch" stand for electrostatic, induction, and exchange, respectively. δSCF_3 is a catchall term for any remaining higher-order electrostatic, induction, and exchange terms. "exch–ind" stands for the exchange correction to induction.

The second-order component can be decomposed as:[39,112]

$$IE_{MP2} - IE_{SCF} = E_{disp}^{(20)} + E_{exch-disp}^{(20)} + E_{elst}^{(12)} + E_{exch-elst}^{(12)} + E_{ind}^{(22)} + E_{exch-ind}^{(22)} + \delta MP2 \tag{6}$$

where "disp" stands for dispersion, "exch–disp" for the exchange correction to dispersion, and $\delta MP2$ is a catchall term for higher-order electrostatic and induction terms. It is important to realize that $E_{disp}^{(20)}$ has identical αα and αβ components: inclusion of $E_{exch-disp}^{(20)}$ introduces spin dependence.

For the third-order terms, eqn (6:35) of Chalasinski and Szczesniak[102] implies that

$$IE_{MP3} - IE_{MP2} = E_{disp}^{(21)} + E_{exch-disp}^{(21)} + E_{elst}^{(13)} + E_{disp}^{(30)} + E_{exch-disp}^{(30)} + \delta MP3 \tag{7}$$

Additional terms will appear at fourth order:

$$IE_{MP4} - IE_{MP3} = E_{disp}^{(22)}(SDQ) + E_{disp}^{(22)}(T) + \ldots \tag{8}$$

At the two least expensive levels of SAPT, SAPT0 and SAPT2, the interaction energy can be decomposed as:

$$IE_{SAPT0} = E_{elst}^{(10)} + E_{exch}^{(10)} + E_{ind}^{(20)} + E_{exch-ind}^{(20)} + E_{disp}^{(20)} + E_{exch-disp}^{(20)} \tag{9}$$

$$IE_{SAPT2} = IE_{SAPT0} + E_{elst}^{(12)} + E_{exch-elst}^{(12)} + E_{ind}^{(22)} + E_{exch-ind}^{(22)} \tag{10}$$

Let us now consider the variable:

$$NDF2 = \frac{E_{disp}^{(2)}}{IE^{(2)}} - 1 = \frac{E_{disp}^{(20)} + E_{exch-disp}^{(20)}}{IE_{ss}^{(2)} + IE_{ab}^{(2)}} - 1$$

$$= \frac{E_{disp}^{(20)} + E_{exch-disp}^{(20)}}{IE_{aa}^{(2)} + IE_{bb}^{(2)} + IE_{ab}^{(2)}} - 1 \tag{11}$$

where $IE^{(2)}$ stands for the MP2 correlation component to the interaction energy, and $IE_{ss}^{(2)}$ and $IE_{ab}^{(2)}$ stand for the same-spin and opposite-spin components thereof, respectively. In a -system dominated by dispersion, NDF2 (non-dispersion fraction at 2nd order) will be close to zero, while in a system with significant nondispersion contributions to the 2nd-order correlation energy, it will typically be positive (correlation corrections to the electrostatic interaction energy tend to be repulsive).

20920 | *Phys. Chem. Chem. Phys.*, 2016, **18**, 20905–20925

This journal is © the Owner Societies 2016

NDF2 can be computed from an MP2 and an SAPT0 calculation in the same basis set. However, let us now consider the following variable that just requires an MP2 or RI-MP2 calculation:

$$\text{CSPI} = \frac{\text{IE}_{ss}^{(2)} - \text{IE}_{ab}^{(2)}}{\text{IE}_{ss}^{(2)} + \text{IE}_{ab}^{(2)}} \quad (12)$$

Over the S66x8 set, with the haVTZ basis set, we found that NDF2 and CSPI (correlation spin polarization index) have a squared correlation coefficient of no less than 0.991 (see Table S1 in ESI†). We may therefore safely conclude that they contain the same chemical information.

For a system where the interaction energy is dominated by $E_{\text{disp}}^{(20)}$, CSPI will approach zero; in systems where non-dispersion factors play a role in the correlation part of the interaction energy, CSPI will depart from zero. However, for highly stretched systems, absolute values of the same-spin and opposite component may be so small that CSPI suddenly flips sign. In order to avoid this problem, we will instead consider

$$\text{DEBC} = \sqrt{\frac{\text{CSPI}^2}{1 + \text{CSPI}^2}} = \sqrt{\frac{1}{2} - \frac{\text{IE}_{ss}^{(2)} \text{IE}_{ab}^{(2)}}{\left(\text{IE}_{ss}^{(2)}\right)^2 + \left(\text{IE}_{ab}^{(2)}\right)^2}} \quad (13)$$

where the acronym stands for dispersion-electrostatic balance in correlation. In the long-distance limit for, e.g., hydrogen-bonded complexes, the rapidly decaying dispersive component will be small compared to the more slowly decaying nondispersion terms (which are typically repulsive in the correlation component), and as a result the second term will strive to $-\frac{1}{2}$ and DEBC will approach unity. DEBC thus moves on a scale from 0 for purely dispersive (e.g., argon dimer) to 1 for purely nondispersive.

However, at very long distance in systems dominated by nondispersion effects (e.g., acetic acid dimer), $\text{IE}^{(2)}$ will be negligible compared to IE_{SCF} and hence DEBC may not be very informative anymore. We will instead consider two additional indices. One is the fraction of the interaction energy accounted for at the Hartree–Fock level

$$\%\text{HF} = \frac{(100\%) \times \text{IE}_{\text{SCF}}}{\text{IE}_{\text{SCF}} + \text{IE}_{ss}^{(2)} + \text{IE}_{ab}^{(2)} + \text{IE}_{\text{HLC}}} \approx \frac{(100\%) \times \text{IE}_{\text{SCF}}}{\text{IE}_{\text{SCF}} + \text{IE}_{ss}^{(2)} + \text{IE}_{ab}^{(2)}} \quad (14)$$

For systems dominated by electrostatic effects (e.g., H_2O dimer at long distance), %HF will approach 100%; for systems where the primary HF-level component is exchange repulsion (e.g. alkane dimers), %HF will be negative.

A second index is the fraction of the interaction energy accounted for by post-MP2 correlation effects:

$$\%\text{HLC} = \frac{(100\%) \times \text{IE}_{\text{HLC}}}{\text{IE}_{\text{SCF}} + \text{IE}_{ss}^{(2)} + \text{IE}_{ab}^{(2)} + \text{IE}_{\text{HLC}}} \quad (15)$$

This index will typically be low for systems dominated by electrostatic effects. For systems dominated by London dispersion (e.g., alkane dimers), it is empirically found to be small as well, since an error compensation appears to take place between neglect of (attractive) connected triple excitations and neglect of (typically repulsive) third- and fourth-order double excitations. In the S66x8 set, large values of %HLC are seen for π-stacking interactions.

In short, by consideration of three indices derived from the calculated interaction energy, one can infer the dominant interaction type in a system even without resorting to SAPT calculations.

A complete tabulation, complete with the Hobza disp/elec ratio[9] of values for all the S66x8 systems is given in the ESI.† In Table 16, we present data for some representative systems.

First, let us consider the acetic acid dimer with its strong double hydrogen bond. The Hobza ratio is solidly in the electrostatic range. CSPI and therefore DEBC are large, %HLC is close to zero, and as the dimer is pulled apart, the %SCF in the interaction energy approach is 100%. At long distance, the interaction energy indeed behaves similar to the R^{-3} power law expected for dipole–dipole electrostatic interactions.

Next, the stacked benzene dimer. Here, we find a small negative CSPI and a large HLC fraction. The HF fraction is negative throughout, consisting effectively of exchange repulsion. Long-range behavior is in fact not dissimilar to the R^{-5} expected for a quadrupole–quadrupole interaction.

For the stacked uracil dimer, we see something similar at short range, but at longer distances we see HLC becoming fairly unimportant, CSPI rising, and HF capturing an increasing positive fraction of the interaction energy. This reflects that, unlike the benzene dimer, there is a dipole–dipole interaction at longer distances in the uracil dimer.

For pentane dimer, CSPI stays small throughout, as does the %HLC. The HF contribution is repulsive but tapers off quickly at long distances, where the behavior is dominated by the London interaction.

In the mixed-influence benzene–water complex, on the other hand, CSPI is near zero at short distances but goes up at long distances (where a dipole–quadrupole interaction dominates), while the HLC fraction is substantial at short distances but tapers off to near zero at longer ones, and the HF fraction is small at short distances but approaches unity in the long-distance regime.

Conclusions

We have presented a revision of the S66x8 dataset by means of explicitly correlated methods, combining basis set limit MP2-F12 energies with CCSD(Tc$_{\text{sc}}$)-F12b/cc-pVDZ-F12 high level corrections. Based on assessments for smaller datasets, we deem our results reliable to about 0.05 kcal mol^{-1} RMS. The RMS deviation from the original S66x8 reference data is 0.11 kcal mol^{-1}, comparable to the performance of the best DFT levels considered here.

Most levels of DFT perform quite poorly in the absence of dispersion corrections: somewhat surprisingly, that is even the case for the double hybrids and for dRPA75. Even the simple D2 empirical dispersion leads to substantial improvement, especially for dRPA75-D2 ($s_6 = 0.31$, RMSD = 0.13 kcal mol^{-1})

This journal is © the Owner Societies 2016

Phys. Chem. Chem. Phys., 2016, 18, 20905–20925 | 20921

Table 16 Indices for type of noncovalent interaction, and their evolution along the dissociation curve, for selected systems in the S66 set. Interaction energies in kcal mol^{-1} added for clarity

	NDF2	CSPI	DEBC	Hobza ratio disp/(elec + ind)	%HF	%HLC	IE (kcal mol^{-1})
H-bond$\cdots$(CH$_3$COOH)$_2$							
$20\cdots0.90r_e$	2.656	1.046	0.723	0.166	80.5	−2.0	−17.970
$20\cdots0.95r_e$	2.515	1.037	0.720	0.170	85.0	−2.2	−19.228
$20\cdots1.00r_e$	2.440	1.045	0.723	0.173	87.9	−2.4	−19.469
$20\cdots1.05r_e$	2.417	1.068	0.730	0.176	90.1	−2.6	−19.049
$20\cdots1.10r_e$	2.439	1.105	0.742	0.178	91.8	−2.8	−18.219
$20\cdots1.25r_e$	2.760	1.322	0.798	0.180	95.4	−3.1	−14.736
$20\cdots1.50r_e$	4.841	2.467	0.927	0.167	99.3	−3.2	−9.289
$20\cdots2.00r_e$	−6.091	−3.304	0.957	0.126	105.1	−2.9	−3.611
π-stack (C$_6$H$_6$)$_2$ parallel displaced							
$24\cdots0.90r_e$	0.028	−0.067	0.067	1.535	−185.2	53.8	−0.105
$24\cdots0.95r_e$	0.020	−0.061	0.061	2.062	−111.4	39.5	−2.016
$24\cdots1.00r_e$	0.014	−0.056	0.056	2.869	−75.9	32.5	−2.725
$24\cdots1.05r_e$	0.008	−0.052	0.051	4.229	−55.9	28.5	−2.813
$24\cdots1.10r_e$	0.003	−0.048	0.048	6.930	−43.7	26.1	−2.607
$24\cdots1.25r_e$	−0.014	−0.042	0.042	−18.003	−28.1	22.7	−1.578
$24\cdots1.50r_e$	−0.043	−0.044	0.044	−4.045	−29.5	21.7	−0.515
$24\cdots2.00r_e$	−0.083	−0.064	0.064	−2.242	−53.0	23.1	−0.072
π-stack (uracil)$_2$ stacked							
$26\cdots0.90r_e$	0.174	0.045	0.045	0.963	−68.1	18.4	−7.976
$26\cdots0.95r_e$	0.167	0.054	0.054	1.069	−23.4	12.8	−9.640
$26\cdots1.00r_e$	0.164	0.064	0.064	1.157	−0.4	9.8	−9.976
$26\cdots1.05r_e$	0.164	0.075	0.074	1.220	13.7	8.0	−9.590
$26\cdots1.10r_e$	0.166	0.086	0.086	1.255	23.2	6.7	−8.848
$26\cdots1.25r_e$	0.193	0.128	0.127	1.209	40.1	4.4	−6.217
$26\cdots1.50r_e$	0.301	0.227	0.222	0.927	55.7	2.5	−3.196
$26\cdots2.00r_e$	0.840	0.647	0.543	0.521	77.9	−0.4	−1.034
London (n-pentane)$_2$							
$34\cdots0.90r_e$	0.079	−0.015	0.015	2.216	−268.8	11.3	−2.919
$34\cdots0.95r_e$	0.064	−0.014	0.014	2.804	−138.9	5.9	−3.674
$34\cdots1.00r_e$	0.053	−0.013	0.013	3.575	−85.8	3.8	−3.820
$34\cdots1.05r_e$	0.043	−0.012	0.012	4.601	−57.4	2.7	−3.651
$34\cdots1.10r_e$	0.034	−0.011	0.011	5.982	−40.3	2.1	−3.337
$34\cdots1.25r_e$	0.017	−0.008	0.008	14.297	−16.0	1.7	−2.257
$34\cdots1.50r_e$	0.003	−0.005	0.005	185.803	−4.7	2.2	−1.066
$34\cdots2.00r_e$	−0.003	−0.003	0.003	−42.381	−2.6	3.5	−0.278
π-stack plus dipole–quadrupole: (C$_6$H$_6$)$_2$ T-shaped							
$47\cdots0.90r_e$	0.082	−0.018	0.018	1.470	−135.8	35.8	−1.657
$47\cdots0.95r_e$	0.076	−0.010	0.010	1.735	−70.7	25.3	−2.603
$47\cdots1.00r_e$	0.072	−0.004	0.004	2.014	−39.0	20.3	−2.898
$47\cdots1.05r_e$	0.070	0.003	0.003	2.290	−20.4	17.3	−2.853
$47\cdots1.10r_e$	0.070	0.009	0.009	2.539	−8.3	15.5	−2.643
$47\cdots1.25r_e$	0.072	0.027	0.027	2.955	10.7	12.8	−1.804
$47\cdots1.50r_e$	0.088	0.052	0.052	2.668	23.2	11.4	−0.856
$47\cdots2.00r_e$	0.136	0.095	0.095	1.783	34.6	9.9	−0.237
Mixed-influence: (C$_6$H$_6$)$\cdots$H$_2$O							
$54\cdots0.90r_e$	0.194	0.048	0.048	0.732	−30.3	14.9	−2.766
$54\cdots0.95r_e$	0.206	0.063	0.063	0.739	5.9	10.5	−3.186
$54\cdots1.00r_e$	0.221	0.080	0.080	0.731	25.5	8.2	−3.250
$54\cdots1.05r_e$	0.241	0.099	0.099	0.711	38.0	6.8	−3.121
$54\cdots1.10r_e$	0.266	0.121	0.120	0.680	46.9	5.9	−2.896
$54\cdots1.25r_e$	0.374	0.203	0.199	0.558	63.3	4.5	−2.105
$54\cdots1.50r_e$	0.717	0.439	0.402	0.375	78.0	3.7	−1.160
$54\cdots2.00r_e$	4.515	2.948	0.947	0.193	92.7	3.2	−0.419

and for DSD-PBEP86-D2 ($s_6 = 0.27$, RMSD = 0.15 kcal mol^{-1}). Below the fifth rung, ωB97X-V without NL, adding D2 is seen as the best performer ($s_6 = 0.73$, RMSD = 0.31 kcal mol^{-1}).

The D3BJ correction leads to further improvements for GGAs and hybrids, much less so for fifth-rung functionals. (D3BJ parameters for a number of additional functionals were optimized in this work.) Significantly, the optimized s_8 coefficient for the R^{-8} term is close to zero for the double hybrids and dRPA75, or needs to be fixed at zero to get a stable fit. In contrast, for the APF functional (which is constructed to be dispersion-free on average), $s_6 = 1.776$, while for MP2, $s_6 = -3.351$. This illustrates that the primary benefit of fifth-rung functionals for noncovalent

20922 | *Phys. Chem. Chem. Phys.*, 2016, **18**, 20905–20925

This journal is © the Owner Societies 2016

interactions lies in the handling of medium-range interactions: in straight MP2, overcorrection takes place in that region, which is remedied in the case of dRPA75-D3BJ by higher-order correlation corrections, and in the double hybrids by the use of a mixture of GGA and KS-MP2 correlation. dRPA75-D3BJ actually falls below the RMSD = 0.10 kcal mol^{-1} threshold. B3LYP-D3BJ performs surprisingly well at RMSD = 0.20 kcal mol^{-1}.

Considering S66x8 in tandem with the amino acid conformers illustrates why it is worthwhile to consider multiple benchmarks for evaluation lower-level methods: dRPA75-D3BJ performs well on both sets, dRPA75 and dRPA75-D2 each on only one set.

A nonlocal (Vydrov–Van Voorhis 2010, or VV10) correlation model performs less well than D3BJ for some GGAs and hybrids, while it is superior for the double hybrids, particularly for DSD-PBEP86-NL, with RMSD = 0.12 kcal mol^{-1}. Among the range-separated hybrids, ωB97X-V stands out, with RMSD = 0.23 kcal mol^{-1}.

A caveat is due here: the benchmark study in the present paper only concerns noncovalent interactions and any conclusions reached about the performance of specific DFT methods are not necessarily applicable to other properties. It is however worth mentioning that one of the best performers for the S66x8 benchmark, namely the DSD-PBEP86-D3BJ double hybrid,[79,80] also was found to yield outstanding performance for general thermochemistry[79,80] and reaction barrier heights,[79,80] as well as for vibrational frequencies.[111] The same remarks apply, to a lesser extent, for the B2GP-PLYP-D2 double hybrid.[78] The computational surcharge for such approaches is actually fairly modest if the RI-MP2 (resolution of the identity MP2) method[32,33] can be used for the MP2-like step.

Informative as SAPT may be about the character of a given interaction, a collection of three energetically based indices offer similar information. Two of those are the percentages of Hartree–Fock and of post-MP2 correlation effects in the interaction energy: the third

$$\mathrm{DEBC} = \sqrt{\frac{1}{2} - \frac{\mathrm{IE}_{ss}^{(2)}\mathrm{IE}_{ab}^{(2)}}{\left(\mathrm{IE}_{ss}^{(2)}\right)^2 + \left(\mathrm{IE}_{ab}^{(2)}\right)^2}}$$

describes the character of the MP2 correlation contribution, ranging from 0 (purely dispersion) to 1 (purely other effects).

In the context of CCSD(T)-F12b calculations, we propose (Tb), namely an improved, parameter-free scaling for the (T) contribution based on the $E_{\mathrm{corr}}[\mathrm{CCSD\text{-}F12b}]/E_{\mathrm{corr}}[\mathrm{CCSD}]$ rather than the $E_{\mathrm{corr}}[\mathrm{MP2\text{-}F12}]/E_{\mathrm{corr}}[\mathrm{MP2}]$ ratio. Similarly, we propose (Tc) for CCSD(F12*)(T) calculations, where the scaling is done by the $E_{\mathrm{corr}}[\mathrm{CCSD(F12*)}]/E_{\mathrm{corr}}[\mathrm{CCSD}]$ ratio instead.

Regarding the accuracy of wavefunction ab $initio$ methods, the several flavors of MP2 and SCS-MP2 methods have again shown that they can be parametrized for a specific kind of interaction, but at the cost of degrading the other interactions. While MP3 overcorrects, MP2.5, averaging the MP2 and MP3 values, yields excellent performance. Uncorrected CCSD yields no adequate return for the additional computational effort: similar to dRPA75, however, adding in a D2 correction to

compensate for the missing (T) results in an excellent RMSD = 0.16 kcal mol^{-1} (for s_6 = 0.228); even further improvement at zero added cost is possible through SCS(MI)CCSD, or even simple overall scaling of the CCSD correlation energy.

Finally, with the relatively small cc-pVDZ-F12 basis set, CCSD(F12*) has a small but significant edge over CCSD-F12b, particularly for multiply H-bonded systems.

Acknowledgements

References

1 K. E. Riley and P. Hobza, $Wiley\ Interdisc.\ Rev.:\ Comput.\ Mol.\ Sci.$, 2011, **1**, 3–17.
2 K. E. Riley and P. Hobza, $Acc.\ Chem.\ Res.$, 2013, **46**, 927–936.
3 M. J. Robertson, J. Tirado-Rives and W. L. Jorgensen, $J.\ Chem.\ Theory\ Comput.$, 2015, **11**, 3499–3509.
4 J. J. P. Stewart, $J.\ Mol.\ Model.$, 2013, **19**, 1–32.
5 B. P. Martin, C. J. Brandon, J. J. P. Stewart and S. B. Braun-Sand, $Proteins:\ Struct.,\ Funct.,\ Bioinf.$, 2015, **83**, 1427–1435.
6 G. Jansen, $Wiley\ Interdisc.\ Rev.:\ Comput.\ Mol.\ Sci.$, 2014, **4**, 127–144.
7 E. G. Hohenstein and C. D. Sherrill, $Wiley\ Interdisc.\ Rev.:\ Comput.\ Mol.\ Sci.$, 2012, **2**, 304–326.
8 K. Szalewicz, $Wiley\ Interdisc.\ Rev.:\ Comput.\ Mol.\ Sci.$, 2012, **2**, 254–272.
9 J. Řezáč, K. E. Riley and P. Hobza, $J.\ Chem.\ Theory\ Comput.$, 2011, **7**, 2427–2438.
10 I. G. Kaplan, $Intermolecular\ Interactions$, John Wiley & Sons, Ltd, Chichester, UK, 2006.
11 P. Jurecka, J. Sponer, J. Cerný and P. Hobza, $Phys.\ Chem.\ Chem.\ Phys.$, 2006, **8**, 1985–1993.
12 M. S. Marshall, L. A. Burns and C. D. Sherrill, $J.\ Chem.\ Phys.$, 2011, **135**, 194102.
13 J. Řezáč, K. E. Riley and P. Hobza, $J.\ Chem.\ Theory\ Comput.$, 2011, **7**, 3466–3470.
14 J. Řezáč, P. Jurečka, K. E. Riley, J. Černý, H. Valdes, K. Pluháčková, K. Berka, T. Řezáč, M. Pitoňák, J. Vondrášek and P. Hobza, $Collect.\ Czech.\ Chem.\ Commun.$, 2008, **73**, 1261–1270, see also: http://www.begdb.com.
15 J. Aragó, E. Ortí and J. C. Sancho-García, $J.\ Chem.\ Theory\ Comput.$, 2013, **9**, 3437–3443.
16 F. Yu, $J.\ Chem.\ Theory\ Comput.$, 2014, **10**, 4400–4407.

17 L. Goerigk, H. Kruse and S. Grimme, *ChemPhysChem*, 2011, **12**, 3421–3433.

18 K. E. Riley, J. A. Platts, J. Řezáč, P. Hobza and J. G. Hill, *J. Phys. Chem. A*, 2012, **116**, 4159–4169.

19 J. A. Platts, J. G. Hill, K. E. Riley, J. Řezáč and P. Hobza, *J. Chem. Theory Comput.*, 2013, **9**, 330–337.

20 M. J. Turner, S. Grabowsky, D. Jayatilaka and M. A. Spackman, *J. Phys. Chem. Lett.*, 2014, 4249–4255.

21 L. Kong, F. A. Bischoff and E. F. Valeev, *Chem. Rev.*, 2012, **112**, 75–107.

22 C. Hättig, W. Klopper, A. Köhn and D. P. Tew, *Chem. Rev.*, 2012, **112**, 4–74.

23 S. Ten-no, *Chem. Phys. Lett.*, 2004, **398**, 56–61.

24 K. A. Peterson, D. A. Dixon and H. Stoll, *J. Phys. Chem. A*, 2012, **116**, 9777–9782.

25 J. M. L. Martin and M. K. Kesharwani, *J. Chem. Theory Comput.*, 2014, **10**, 2085–2090.

26 B. Brauer, M. K. Kesharwani and J. M. L. Martin, *J. Chem. Theory Comput.*, 2014, **10**, 3791–3799.

27 K. A. Peterson, M. K. Kesharwani and J. M. L. Martin, *Mol. Phys.*, 2015, **113**, 1551–1558.

28 H.-J. Werner, P. J. Knowles, G. Knizia, F. R. Manby, M. Schütz, P. Celani, T. Korona, R. Lindh, A. Mitrushenkov, G. Rauhut, K. R. Shamasundar, T. B. Adler, R. D. Amos, A. Bernhardsson, A. Berning, D. L. Cooper, M. J. O. Deegan, A. J. Dobbyn, F. Eckert, E. Goll, C. Hampel, A. Hesselman, G. Hetzer, T. Hrenar, G. Jansen, C. Köppl, Y. Liu, A. W. Lloyd, R. A. Mata, A. J. May, S. J. McNicholas, W. Meyer, M. E. Mura, A. Nicklass, D. P. O'Neill, P. Palmieri, D. Peng, K. Pflüger, R. M. Pitzer, M. Reiher, T. Shiozaki, H. Stoll, A. J. Stone, R. Tarroni, T. Thorsteinsson and M. Wang, *MOLPRO, Version 2012.1, a Package of Ab Initio Programs*, University of Cardiff Chemistry Consultants (UC3), Cardiff, Wales, UK, 2012, see also: https://www.molpro.net.

29 F. Furche, R. Ahlrichs, C. Hättig, W. Klopper, M. Sierka and F. Weigend, *Wiley Interdiscip. Rev.: Comput. Mol. Sci.*, 2013, **4**, 91–100, see also: http://www.turbomole.com.

30 M. J. Frisch, G. W. Trucks, H. B. Schlegel, G. E. Scuseria, M. A. Robb, J. R. Cheeseman, G. Scalmani, V. Barone, B. Mennucci, G. A. Petersson, H. Nakatsuji, M. Caricato, X. Li, H. P. Hratchian, A. F. Izmaylov, J. Bloino, G. Zheng, J. L. Sonnenberg, M. Hada, M. Ehara, K. Toyota, R. Fukuda, J. Hasegawa, M. Ishida, T. Nakajima, Y. Honda, O. Kitao, H. Nakai, T. Vreven, J. A. Montgomery, Jr., J. E. Peralta, F. Ogliaro, M. Bearpark, J. J. Heyd, E. Brothers, K. N. Kudin, V. N. Staroverov, R. Kobayashi, J. Normand, K. Raghavachari, A. P. Rendell, J. C. Burant, S. S. Iyengar, J. Tomasi, M. Cossi, N. Rega, M. J. Millam, M. Klene, J. E. Knox, J. B. Cross, V. Bakken, C. Adamo, J. Jaramillo, R. Gomperts, R. E. Stratmann, O. Yazyev, A. J. Austin, R. Cammi, C. Pomelli, J. W. Ochterski, R. L. Martin, K. Morokuma, V. G. Zakrzewski, G. A. Voth, P. Salvador, J. J. Dannenberg, S. Dapprich, A. D. Daniels, Ö. Farkas, J. B. Foresman, J. V. Ortiz, J. Cioslowski and D. J. Fox, *Gaussian 09 Rev. D01.*, Gaussian, Inc., Wallingford, CT, 2012, see also: http://www.gaussian.com.

31 F. Neese, *Wiley Interdiscip. Rev.: Comput. Mol. Sci.*, 2012, **2**, 73–78, see also: https://orcaforum.cec.mpg.de.

32 F. Weigend and M. Häser, *Theor. Chem. Acc.*, 1997, **97**, 331–340.

33 R. A. Kendall and H. A. Früchtl, *Theor. Chem. Acc.*, 1997, **97**, 158–163.

34 T. H. Dunning, *J. Chem. Phys.*, 1989, **90**, 1007.

35 R. A. Kendall, T. H. Dunning and R. J. Harrison, *J. Chem. Phys.*, 1992, **96**, 6796.

36 D. E. Woon and T. H. Dunning, *J. Chem. Phys.*, 1993, **98**, 1358.

37 K. A. Peterson, D. E. Woon and T. H. Dunning, *J. Chem. Phys.*, 1994, **100**, 7410.

38 J. E. Del Bene, *J. Phys. Chem.*, 1993, **97**, 107–110.

39 T. M. Parker, L. A. Burns, R. M. Parrish, A. G. Ryno and C. D. Sherrill, *J. Chem. Phys.*, 2014, **140**, 094106.

40 E. Papajak, J. Zheng, X. Xu, H. R. Leverentz and D. G. Truhlar, *J. Chem. Theory Comput.*, 2011, **7**, 3027–3034.

41 F. Weigend and R. Ahlrichs, *Phys. Chem. Chem. Phys.*, 2005, **7**, 3297.

42 D. Rappoport and F. Furche, *J. Chem. Phys.*, 2010, **133**, 134105.

43 F. Weigend, *J. Comput. Chem.*, 2008, **29**, 167–175.

44 C. Hättig, *Phys. Chem. Chem. Phys.*, 2005, **7**, 59.

45 K. A. Peterson, T. B. Adler and H.-J. Werner, *J. Chem. Phys.*, 2008, **128**, 084102.

46 K. E. Yousaf and K. A. Peterson, *J. Chem. Phys.*, 2008, **129**, 184108.

47 K. E. Yousaf and K. A. Peterson, *Chem. Phys. Lett.*, 2009, **476**, 303–307.

48 J. G. Hill, K. A. Peterson, G. Knizia and H.-J. Werner, *J. Chem. Phys.*, 2009, **131**, 194105.

49 T. B. Adler, G. Knizia and H.-J. Werner, *J. Chem. Phys.*, 2007, **127**, 221106.

50 J. Noga and J. Šimunek, *Chem. Phys.*, 2009, **356**, 1–6.

51 O. Marchetti and H.-J. Werner, *Phys. Chem. Chem. Phys.*, 2008, **10**, 3400.

52 O. Marchetti and H.-J. Werner, *J. Phys. Chem. A*, 2009, **113**, 11580–11585.

53 S. Grimme, *J. Chem. Phys.*, 2003, **118**, 9095.

54 A. Szabados, *J. Chem. Phys.*, 2006, **125**, 214105.

55 S. Grimme, L. Goerigk and R. F. Fink, *Wiley Interdiscip. Rev.: Comput. Mol. Sci.*, 2012, **2**, 886–906.

56 R. F. Fink, *J. Chem. Phys.*, 2010, **133**, 174113.

57 J. P. Perdew and K. Schmidt, *AIP Conf. Proc.*, 2001, **577**, 1–20.

58 A. D. Becke, *Phys. Rev. A: At., Mol., Opt. Phys.*, 1988, **38**, 3098–3100.

59 J. P. Perdew, *Phys. Rev. B: Condens. Matter Mater. Phys.*, 1986, **33**, 8822–8824.

60 C. Lee, W. Yang and R. G. Parr, *Phys. Rev. B: Condens. Matter Mater. Phys.*, 1988, **37**, 785–789.

61 J. P. Perdew, K. Burke and M. Ernzerhof, *Phys. Rev. Lett.*, 1996, **77**, 3865–3868.

62 J. Tao, J. Perdew, V. Staroverov and G. Scuseria, *Phys. Rev. Lett.*, 2003, **91**, 146401.

63 Y. Zhao and D. G. Truhlar, *Theor. Chem. Acc.*, 2008, **120**, 215–241.

64 A. D. Becke, *J. Chem. Phys.*, 1993, **98**, 1372.

65 A. D. Becke, *J. Chem. Phys.*, 1993, **98**, 5648.

66 P. J. Stephens, F. J. Devlin, C. F. Chabalowski and M. J. Frisch, *J. Phys. Chem.*, 1994, **98**, 11623–11627.

67 Y. Wang and J. P. Perdew, *Phys. Rev. B: Condens. Matter Mater. Phys.*, 1991, **44**, 13298–13307.

68 C. Adamo and V. Barone, *J. Chem. Phys.*, 1999, **110**, 6158.

69 S. Grimme, *J. Phys. Chem. A*, 2005, **109**, 3067–3077.

70 M. M. Quintal, A. Karton, M. A. Iron, A. D. Boese and J. M. L. Martin, *J. Phys. Chem. A*, 2006, **110**, 709–716.

71 A. Austin, G. A. Petersson, M. J. Frisch, F. J. Dobek, G. Scalmani and K. Throssell, *J. Chem. Theory Comput.*, 2012, **8**, 4989–5007.

72 R. Peverati and D. G. Truhlar, *J. Phys. Chem. Lett.*, 2011, **2**, 2810–2817.

73 T. Yanai, D. P. Tew and N. C. Handy, *Chem. Phys. Lett.*, 2004, **393**, 51–57.

74 O. A. Vydrov and G. E. Scuseria, *J. Chem. Phys.*, 2006, **125**, 234109.

75 Y.-S. Lin, G.-D. Li, S.-P. Mao and J.-D. Chai, *J. Chem. Theory Comput.*, 2013, **9**, 263–272.

76 N. Mardirossian and M. Head-Gordon, *Phys. Chem. Chem. Phys.*, 2014, **16**, 9904–9924.

77 S. Grimme, *J. Chem. Phys.*, 2006, **124**, 034108.

78 A. Karton, A. Tarnopolsky, J.-F. Lamère, G. C. Schatz and J. M. L. Martin, *J. Phys. Chem. A*, 2008, **112**, 12868–12886.

79 S. Kozuch and J. M. L. Martin, *Phys. Chem. Chem. Phys.*, 2011, **13**, 20104–20107.

80 S. Kozuch and J. M. L. Martin, *J. Comput. Chem.*, 2013, **34**, 2327–2344.

81 P. D. Mezei, G. I. Csonka, A. Ruzsinszky and M. Kállay, *J. Chem. Theory Comput.*, 2015, **11**, 4615–4626.

82 H. Eshuis, J. E. Bates and F. Furche, *Theor. Chem. Acc.*, 2012, **131**, 1084.

83 J. Klimeš and A. Michaelides, *J. Chem. Phys.*, 2012, **137**, 120901.

84 S. Grimme, *J. Comput. Chem.*, 2006, **27**, 1787–1799.

85 T. Schwabe and S. Grimme, *Phys. Chem. Chem. Phys.*, 2007, **9**, 3397–3406.

86 S. Grimme, J. Antony, S. Ehrlich and H. Krieg, *J. Chem. Phys.*, 2010, **132**, 154104.

87 S. Grimme, S. Ehrlich and L. Goerigk, *J. Comput. Chem.*, 2011, **32**, 1456–1465.

88 M. J. D. Powell, *The BOBYQA algorithm for bound constrained optimization without derivatives (DAMPT Report 2009/NA06)*, Department of Applied Mathematics and Theoretical Physics, University of Cambridge, UK, 2009, see also: http://en.wikipedia.org/wiki/BOBYQA [Retrieved February 29, 2016].

89 O. A. Vydrov and T. Van Voorhis, *J. Chem. Phys.*, 2010, **133**, 244103.

90 W. Hujo and S. Grimme, *J. Chem. Theory Comput.*, 2011, **7**, 3866–3871.

91 M. K. Kesharwani, A. Karton and J. M. L. Martin, *J. Chem. Theory Comput.*, 2016, **12**, 444–454.

92 J. M. Turney, A. C. Simmonett, R. M. Parrish, E. G. Hohenstein, F. A. Evangelista, J. T. Fermann, B. J. Mintz, L. A. Burns, J. J. Wilke, M. L. Abrams, N. J. Russ, M. L. Leininger, C. L. Janssen, E. T. Seidl, W. D. Allen, H. F. Schaefer, R. A. King, E. F. Valeev, C. D. Sherrill and T. D. Crawford, *Wiley Interdiscip. Rev.: Comput. Mol. Sci.*, 2012, **2**, 556–565.

93 A. Karton and J. M. L. Martin, *Theor. Chem. Acc.*, 2005, **115**, 330–333.

94 D. W. Schwenke, *J. Chem. Phys.*, 2005, **122**, 14107.

95 D. S. Ranasinghe and G. A. Petersson, *J. Chem. Phys.*, 2013, **138**, 144104.

96 C. Hättig, D. P. Tew and A. Köhn, *J. Chem. Phys.*, 2010, **132**, 231102.

97 T. Takatani, E. G. Hohenstein, M. Malagoli, M. S. Marshall and C. D. Sherrill, *J. Chem. Phys.*, 2010, **132**, 144104.

98 A. Halkier, H. Koch, P. Jørgensen, O. Christiansen, I. M. B. Nielsen and T. Helgaker, *Theor. Chem. Acc.*, 1997, **97**, 150–157.

99 L. A. Burns, M. S. Marshall and C. D. Sherrill, *J. Chem. Theory Comput.*, 2014, **10**, 49–57.

100 A. Hesselmann, *J. Chem. Phys.*, 2008, **128**, 144112.

101 R. A. DiStasio, G. von Helden, R. P. Steele and M. Head-Gordon, *Chem. Phys. Lett.*, 2007, **437**, 277–283.

102 G. Chałasiński and M. M. Szcześniak, *Mol. Phys.*, 1988, **63**, 205–224.

103 A. Szabo and N. S. Ostlund, *J. Chem. Phys.*, 1977, **67**, 4351.

104 R. Sedlak, K. E. Riley, J. Řezáč, M. Pitoňák and P. Hobza, *ChemPhysChem*, 2013, **14**, 698–707.

105 M. Pitoňák and A. Heßelmann, *J. Chem. Theory Comput.*, 2010, **6**, 168–178.

106 J. Řezáč, K. E. Riley and P. Hobza, *J. Chem. Theory Comput.*, 2014, **10**, 1359–1360.

107 J. Toulouse, W. Zhu, A. Savin, G. Jansen and J. G. Ángyán, *J. Chem. Phys.*, 2011, **135**, 084119.

108 G. E. Scuseria, T. M. Henderson and D. C. Sorensen, *J. Chem. Phys.*, 2008, **129**, 231101.

109 D. Gruzman, A. Karton and J. M. L. Martin, *J. Phys. Chem. A*, 2009, **113**, 11974–11983.

110 J. M. L. Martin, *J. Phys. Chem. A*, 2013, **117**, 3118–3132.

111 M. K. Kesharwani, B. Brauer and J. M. L. Martin, *J. Phys. Chem. A*, 2015, **119**, 1701–1714.

112 R. M. Parrish, T. M. Parker and C. D. Sherrill, *J. Chem. Theory Comput.*, 2014, **10**, 4417–4431.